



Technische Universiteit Delft  
Faculteit Elektrotechniek, Wiskunde en Informatica  
Delft Institute of Applied Mathematics

**Analyse van e-gitaar signalen in tijd- en  
frequentiedomein, in termen van snaar- en  
rand-dynamica**

**(Analysis of e-guitar signals in time and frequency  
domain, in terms of string and boundary dynamics)**

Verslag ten behoeve van het  
Delft Institute of Applied Mathematics  
als onderdeel ter verkrijging

van de graad van

**BACHELOR OF SCIENCE  
in  
TECHNISCHE WISKUNDE**

door

**BART DE KONING**

**Delft, Nederland  
Augustus 2019**





**BSc verslag TECHNISCHE WISKUNDE**

**“Analyse van e-gitaar signalen in tijd- en frequentiedomein, in termen van snaar-  
en rand-dynamica”**

**(Engelse titel: “Analysis of e-guitar signals in time and frequency domain, in  
terms of string and boundary dynamics”)**

Bart de Koning

**Technische Universiteit Delft**

**Begeleider**

Dr.ir. R. van der Toorn

**Overige commissieleden**

Dr. B. Janssens

Drs. E.M. van Elderen

Augustus, 2019

Delft



# Abstract

In this thesis we examine various aspects of the output signal produced by the electrical pickup of an electric guitar. We do this by formulating a model of this output signal based on the one dimensional damped wave equation for the motion of one guitar string and (initially) a simple linear model for the output signal based on this motion. This model is compared to measurements of the output signal of a real guitar and their corresponding spectra. From this comparison it is concluded that the damping term in the damped wave equation is sufficient to roughly describe the decrease in amplitude over time of the envelope in the output signal of an electrical guitar.

The measured guitar signal also displays beating which has been considered to be caused by the interference of parallel and perpendicular modes on the guitar string with slightly differing frequencies. It is shown that the order of magnitude of this difference in frequencies between parallel and perpendicular modes is neither caused by different effective values of the damping coefficient nor by the influence of co-vibrating string boundaries. The last chapter gives a very simple method to introduce beating into the predicted signal. This is done by describing the motion of the string as occurring in a rotating plane in which the radial direction is given by the above mentioned model.



# Contents

<b>1</b>	<b>Introduction</b>	<b>3</b>
<b>2</b>	<b>Preliminaries: Sound, music and the electric guitar</b>	<b>5</b>
2.1	Sound and hearing . . . . .	5
2.2	Music: meaning in sound . . . . .	6
2.2.1	Rhythm and pitch . . . . .	6
2.2.2	Consonance versus dissonance . . . . .	6
2.2.3	Timbre . . . . .	6
2.2.4	Tuning: equal temperament . . . . .	6
2.3	The electric guitar . . . . .	7
2.3.1	Basic anatomy . . . . .	7
2.3.2	The magnetic pickup . . . . .	7
2.3.3	From guitar output to sound . . . . .	8
2.4	Fourier analysis . . . . .	9
2.4.1	Function expansions . . . . .	9
2.4.2	The Fourier transform . . . . .	10
<b>3</b>	<b>The basic model for the electric guitar</b>	<b>13</b>
3.1	The simplest model for a string: the one dimensional ideal wave equation with Homogeneous Dirichlet boundary conditions . . . . .	13
3.1.1	The initial and boundary value problem . . . . .	13
3.1.2	Solution by means of separation of variables . . . . .	14
3.1.3	Properties of the solution to the initial and boundary value problem . . . . .	16
3.2	The pickup . . . . .	17
3.3	Reflection on the assumptions made to obtain this model . . . . .	19
3.4	Parallel and perpendicular modes . . . . .	20
<b>4</b>	<b>Comparing the basic model to measurements</b>	<b>21</b>
4.1	Obtaining parameter values for the Fender Lead III . . . . .	21
4.2	Experimental setup . . . . .	21
4.3	Properties of the wave forms . . . . .	22
4.3.1	Qualitative properties of the wave forms: the envelope, decay and beating . . . . .	22
4.3.2	Quantitative properties of the wave forms: fitting the damping parameter and comparing the measurements to the predicted waveform . . . . .	22
4.4	Properties of the spectra . . . . .	24
4.4.1	Qualitative properties of the spectra . . . . .	24
4.4.2	Quantitative properties of the spectra . . . . .	25
<b>5</b>	<b>String boundaries modelled by oscillators</b>	<b>29</b>
5.1	Boundary conditions . . . . .	29
5.1.1	Equation of motion for the boundaries . . . . .	29
5.1.2	Separation of variables . . . . .	31
5.1.3	A remark on the newly found basis . . . . .	33
5.2	Influence on the spectrum . . . . .	33

<b>6</b>	<b>Rotation of the plane of string vibration</b>	<b>37</b>
6.1	Derivation of the new signal model . . . . .	38
6.2	Properties of the new signal model . . . . .	39
6.3	Predicted signal . . . . .	39
<b>7</b>	<b>Conclusion and discussion</b>	<b>41</b>
7.1	Findings . . . . .	41
7.1.1	Background . . . . .	41
7.1.2	Basic model of the guitar, capturing the most essential ingredients . . . .	41
7.1.3	The damping parameter: explanation of the loss of amplitude over time, refutation of the hypothesis that it can explain the envelope modulation .	42
7.1.4	Refutation of co-vibrating boundaries hypothesis as explanation of the envelope modulation . . . . .	42
7.1.5	Explanation of the envelope modulation by interaction of 3D motion and pickup characteristics . . . . .	43
7.2	Emerged questions . . . . .	43
<b>A</b>	<b>Measurements</b>	<b>45</b>
<b>B</b>	<b>Information content: WAV files</b>	<b>55</b>





# Chapter 1

## Introduction

The introduction of the electric guitar at the beginning of the 20<sup>th</sup> century has had a huge influence on many music genres, like pop, jazz and blues. Since then, guitarists have found that different guitars each have a distinct sound and playability, which makes either one or the other more suitable for a particular genre of music. Many different properties of the guitar go into the way it feels and plays, like the string material and thickness, the scale length (the length of the string between the bridge and the nut) and the material and structural properties of the guitar body.

In a YouTube video called *Gibson Les Paul Vs Fender Stratocaster - Which One Is Better?*, guitar guru Erich Andreas raises the question of what makes these two guitars sound so differently. According to Andreas, many people think that some of the difference in sound is due to differences in the pickups between these guitars. Andreas himself claims the biggest difference in sound comes from the difference in scale length of these guitars [1]. People describe the Les Paul as having ‘a rounder, fatter and thicker sound’, and the Stratocaster as having ‘a transparent, thin or even hollow sound.’

As these metaphoric descriptions of guitar sounds demonstrate, describing perception of sound can be quite elusive. We therefore aim to mainly concern ourselves with quantifying the behaviour of electric guitars based on their properties, and where it is not too complicated (within the context of this mathematical text), we try to make connections with human perception of sound.

The structure of the research described in this text is that of a modelling cycle, a structure often used in mathematical physics. First we construct a mathematical model of a guitar string and the pickup based on the one dimensional wave equation. We then use this model to make predictions of the output of the guitar, which we compare to real world measurements. By means of this comparison, we evaluate whether or not the model has the desired predictive power. This evaluation is based on which phenomena of a real guitar the model describes accurately and which phenomena are not yet accurately predicted by the mathematical model. Based on this comparison, modifications are made to the mathematical model, which is the beginning of a new cycle. This cycle is repeated until the the desired predictive power of the model is reached, or at least as far as this is possible in the period of about 3 months available for this project.

In the modelling cycle for mathematical physics, pure mathematics is a tool used to create insight into physical phenomena. We will therefore not much be concerned with the purely mathematical aspect of the mathematical methods used in this text. This concerns things like the question whether or not a certain function is in (the closure of) a newly derived function space. If the application of certain mathematical tools, used with a solid physical foundation, proves helpful in understanding and predicting physical phenomena, therein lies its value for the mathematical physicist.

Once models are developed that sufficiently reproduce the signal of an electric guitar, predictions can be made and tested about the influence of various properties of the guitar to its sound. The outcomes of this research could then be used to design guitars with certain desired playability or sound. It is however mentioned by Fletcher et al. in [2] that in general there is little communication between the craftsmen that build musical instruments and researchers that study musical instruments scientifically. Fletcher et al. therefore give the following motivation

for their studies:

”The first and major role of (scientific research) is therefore to understand all details of sound production of (existing) instruments. This is a really major program (....), an intellectual exercise of great fascination (..).”

(Following Fletcher & Rossing [2, preface]; minor modifications and omissions in parentheses.)

Careful investigation of the waveforms produced by an electric guitar (a Fender Lead III built in 1982) has led us to narrow down our focus to explaining several aspects of this waveform and its spectral content: damping and beating, based on exploring suggestions made by Fletcher et al. in section 5.6 of [2]. Chapters 3 and 4 give a satisfying model of damping as a linear term added to the wave equation, and the order of magnitude of the damping coefficient is obtained by making fits of the measured waveforms. Explaining the beating has proven to be a more challenging and richer topic. We first tested if beating could be explained as the result of the interference of modes parallel and perpendicular to the fret board of the guitar, a suggestion by Fletcher et al. We argue that these parallel and perpendicular modes have slightly different frequencies due to slightly different interactions of the string with the guitar body at the string boundaries. The beating observed in the measurements has a frequency in the order of 1 Hz, so we look for influences on the frequency in the sound spectrum of the guitar sound in this order of magnitude. In chapter 4 we argue that the influence of damping cannot account for the beating frequency observed in the measurements. In chapter 5 we argue based on boundary dynamics that co-oscillating boundaries can probably also not produce beating with the observed frequency (a possibility also suggested by Fletcher et al.). In chapter 6 we present a brief exploration of the wave equation with 2 directions of freedom by mimicking the non-linear effects of the string described by Fletcher et al. We do this by assuming that the plane in which the string oscillates rotates with a constant speed around the axis given by the equilibrium position of the string. This model is then also combined with a more elaborate model of the pickup, which accounts for the fact that the pickup detects movement of the string parallel and perpendicular to the fret board differently.

## Chapter 2

# Preliminaries: Sound, music and the electric guitar

In the following chapters we will develop models for the behaviour and sound of electric guitars. However, to be able to evaluate these models we first need a basic understanding of sound and music and how those are produced and perceived. In this chapter we give an introduction to the concepts of sound, music, hearing, and also a brief introduction into the working of the electric guitar. The last section will give an introduction to Fourier analysis, which is a mathematical theory that heavily underpins the models developed in later chapters.

### 2.1 Sound and hearing

Sound can be described as longitudinal waves of higher and lower density propagating through a physical medium, in the context of hearing usually air. The working of the human ear to perceive this sound is based on recognising the different frequency oscillations and their intensities present in sound. This perception of frequency is called pitch. Although the human ear is sensitive to frequencies roughly between 20 and 20 000 Hz, this sensitivity varies quite strongly within this interval. The human ear is most sensitive in the range of 2 kHz to 5 kHz. Frequencies for which the ear is more sensitive are perceived louder than frequencies for which the ear is less sensitive when both are heard with the same amplitude. This hearing sensitivity also decreases with age. People can sometimes also be aware of sound frequencies below 20 Hz, but these are felt, not heard. Also, when notes lower than 20 Hz are played on an instrument, we can hear the higher frequencies present in the sound produced by the instrument.

Most people can tell the difference between two frequencies if they differ by 0.03% or more. The recognition of proportion of two frequencies is called relative pitch, a skill that most people have and can improve with training. When people can quantify a frequency without the aid of knowing the frequency of a reference tone (usually by specifying it as a musical note, see section 2.2.4), they are said to have the rare ability of ‘perfect’ or ‘absolute’ pitch.

Sound intensity  $I$  can be expressed in power per area, for instance in  $\text{Wm}^{-2}$ . However, sound intensity is often denoted in decibels, a logarithmic scale based on the comparison of  $I$  to the typical human threshold of perception  $I_0$ , which is  $10^{-12} \text{Wm}^{-2}$ . The conversion is given by  $L = 10 \log_{10} \left( \frac{I}{I_0} \right)$  dB. The use of this unit also reflects the fact that most human senses seem to be logarithmic, in the sense that human senses are much better at detecting relative changes than at detecting absolute changes in things like pressure.

The process of hearing is complicated, and the full perception of sound involves very complicated processing by the brain of the signals it receives from the ears. In this text we will therefore focus ourselves on pitch and timbre (see section 2.2.3). One subtle point that is worth mentioning is that of the perception of the phase of an oscillation. It is mostly believed that phase (shift) has a negligible influence on the perception of sound (i.e. people are ‘phase deaf’), but recent studies show that this is not entirely the case, see for instance Štěpánková in [5].

## 2.2 Music: meaning in sound

Now that we have a basic understanding what sound is and how the human ear perceives it, we can introduce some concepts from music theory. Let's say for the sake of simplicity that we can break down musical perception in two main categories: rhythm and pitch.

### 2.2.1 Rhythm and pitch

Rhythm can be thought of as recognizable repetitive patterns in time of pulses of sound which occur with a low enough frequency such that we can make out the individual pulses. These pulses are therefore not perceived as pitch. We won't go in further detail here on rhythm since this text is mainly concerned with pitch. Pitch is also based on the recognition of repetitive sound pulses, but this time the frequency of these pulses is too fast for humans to make out the individual pulses. The pitch is the 'height' we perceive some sounds to have, and it is directly related the frequency of vibration that reach our ears.

### 2.2.2 Consonance versus dissonance

Since Pythagoras (c. 570 – c. 495 BC) people know that two pitches from different frequencies sound nice together when the ratio of their frequencies can be approximated by a fraction of small integers, which we will call a simple fraction. In general we say that the simpler a fraction is the more consonant two frequencies sound together, and the more complicated the fraction is the more dissonant the frequencies sound together. Consonance means that two frequencies sound 'at peace' with each other, while dissonance sounds like there is tension between the two frequencies.<sup>1</sup> Too much dissonance in a sound is unpleasant to listen to, but the interplay between tension and release plays an important role in almost every type of music.

### 2.2.3 Timbre

When any musical instrument plays a note, it produces a frequency that we associate with that note. However, the instrument never produces only a single frequency for one note, but a whole spectrum of frequencies. We identify the note by the lowest frequency produced by the instrument, the so called fundamental frequency. This lowest frequency does not necessarily have the biggest amplitude of all the frequencies present in the sound produced by the instrument. The frequencies above the fundamental frequency are called the overtones, and together with their relative intensities they specify (at least in part) what is called the timbre of the instrument. The timbre makes a note played on a guitar sound different from the same note played on a violin. Timbre is also what most of this text is concerned with: the goal of this text is to produce models that recreate the wave form and corresponding frequency spectrum of the signal of an electric guitar which can be used to predict how certain aspects of the guitar influence the wave form and the frequency spectrum.

### 2.2.4 Tuning: equal temperament

The relationship between musical notes and the corresponding fundamental frequency is quite straightforward. In modern times, the tuning system called 'equal temperament' is the most popular. This system is defined by saying that the note  $A_4$  has a frequency of 440 Hz, and every semitone up or down contributes a factor  $\sqrt[12]{2}$  to the frequency (coming from the fact that in

---

<sup>1</sup>It should be noted that the perception of consonance versus dissonance is dependent on culture and even on context: certain intervals can sound very dissonant in pop but even too consonant in jazz.

western music an octave, the ratio of 1 : 2 between frequencies, is divided into 12 semitones). Hence if a note is  $m$  semitones away from the note  $A_4$ , its (fundamental) frequency is given by

$$f_1 = 440 \cdot 2^{\frac{m}{12}}. \quad (2.1)$$

## 2.3 The electric guitar

### 2.3.1 Basic anatomy

Figure 2.1a shows schematically all the relevant parts of a typical electric guitar. We will mostly be concerned with the strings, whose effective length is measured from the bridge to the nut. The tuners are used to change the tension on the string, which affects the frequencies of the vibrations on the string (see section 3.1). The pickups produce the electrical output signal of the guitar which depends on the motion of the strings. Subsection 2.3.2 gives more detail on how the pickups produce this signal.

Most electric guitars have 6 strings of varying thickness and sometimes also varying material. In general it applies that the heavier the string is, the lower frequency oscillations it produces. The most standard tuning for six-string guitars is shown in table 2.1.

Table 2.1: Standard tuning of a six-string guitar. The open string ground frequencies were calculated using eq. (2.1). The subscripts in the open string note names indicate the octave in which the note is located.

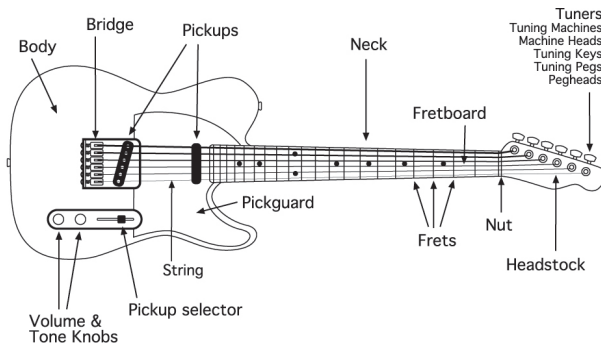
string name	open string note	open string ground frequency (Hz)
high E	$E_4$	329.63
B	$B_3$	246.94
G	$G_3$	196.00
D	$D_3$	146.83
A	$A_2$	110
low E	$E_2$	82.41

In this text we will only be concerned with the highest 3 strings, namely the high E, the B and the G string.

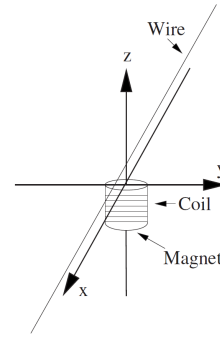
The effective length of the string can be varied by using the frets. When the string is pressed down somewhere on the fret board, the effective string length becomes the distance between the bridge and the nearest fret to the left of where string is pressed as seen from the perspective of fig. 2.1a. When the string is played without pressing it down onto the fret board, the string is called open.

### 2.3.2 The magnetic pickup

As mentioned by Horton et al. in [8], the magnetic pickup is an application of Faraday's law of electromagnetism. In the magnetic pickup, the motion of a ferromagnetic guitar string is converted to an electrical signal by means of electromagnetic induction. For each string, a permanent magnet beneath the string in the pickup produces a magnetic field which is distorted by the presence of the string. The change in distortion of this field by the movement of the string is what induces an electrical current in the coil, see fig. 2.1b. It is also mentioned in [8] that the working of the magnetic pickup introduces certain distortions in the signal and



(a) The various parts of an electric guitar, in this case a Fender Telecaster. In this text we are mostly interested in the string from the the bridge to the nut and the (location of) the pickup [4].



(b) A simple magnetic pickup. The oscillating ferromagnetic wire induces a change in the magnetic flux trough the coil [8].

that the oscillations parallel to the fret board produce a much stronger effect than oscillations perpendicular to the fret board.

As seen in fig. 2.1a, some guitars have multiple pickups. Often the signals of these pickups can be mixed with the pickup selector. For simplicity, in this text we only use one pickup at a time. Some guitars also have a special type of pickup called Humbuckers: this is essentially a pair of pickups placed very close to each other along the string. Often these two pickups that make up the Humbucker pickup can be used separately, as is the case with the guitar used in the experiments described in chapter 4.

To simplify calculations, in this text we will assume that the current produced by the pickup is simply proportional to the speed of the string at the location above the pickup. In chapter 6 we will extend this model slightly to account for the difference in signal produced by the pickup for oscillations perpendicular and parallel to the fret board.

### 2.3.3 From guitar output to sound

Often the process of converting the electrical signal that is produced by the guitar to sound is quite complicated and involves a lot of steps. The most straight forward conversion is by directly connecting the guitar to an amplifier: a device that strengthens the electrical signal and sends it to a speaker. The speaker then produces a sound by moving its cone directly in correspondence to the the voltage of the electrical signal produced by the guitar.

In a typical electrical guitar setup there are a lot of steps between the guitar and the amplifier. These steps involve devices that distort the signal in ways that produce a certain desired timbre. Often amplifiers can perform some of these distortions as well. To obtain the most pure unprocessed signal possible, for the experiments in this text we recorded the signal coming from the guitar directly, see chapter 4.

## 2.4 Fourier analysis

Fourier analysis can be described as the application of concepts from linear algebra to function spaces. Expressing a known function in a linear combination of eigenfunctions is a problem that often pops up in the context of solving linear partial differential equations. The construction of this linear combination involves the use of a properly chosen inner product on the set of eigenfunctions. For an introduction into this topic with a strong theoretical basis see for instance chapter 6 from [12].

### 2.4.1 Function expansions

The Fourier sine series of a function  $f : [0, L] \rightarrow \mathbb{R}$  is given by

$$f(x) \sim \sum_{n=1}^{\infty} C_n \sin\left(\frac{n\pi x}{L}\right), \quad (2.2)$$

where

$$C_n = \frac{2}{L} \int_0^L f(x) \sin\left(\frac{n\pi x}{L}\right) dx. \quad (2.3)$$

We write ‘ $\sim$ ’ in eq. (2.2) since it is not clear that the series on the right always converges to the value  $f(x)$ . In fact, from Haberman in [10] we obtain the following theorem on the Fourier sine series:

**Theorem 1** *For piecewise smooth functions  $f : [0, L] \rightarrow \mathbb{R}$ , on  $[0, L]$  the Fourier sine series of  $f$  is continuous and converges*

1. To  $f$  where  $f$  is continuous,
2. To  $\frac{1}{2}[f(x^+) + f(x^-)]$  where  $f$  has a jump discontinuity.

A piecewise function  $f$  is defined here as a function whose domain can be broken up into finitely many intervals on which  $f$  and  $\frac{df}{dx}$  are both continuous.  $f(x^+)$  and  $f(x^-)$  here denote one-sided limits:

$$f(x^+) = \lim_{x' \uparrow x} f(x'), \quad f(x^-) = \lim_{x' \downarrow x} f(x'). \quad (2.4)$$

By the periodic nature of the Fourier sine series, item 2 of theorem 1 also means that if  $f(0^-) \neq f(L^+)$ , the Fourier sine series of  $f$  converges to  $\frac{1}{2}[f(0^-) + f(L^+)]$  in  $x = 0$  and  $x = L$ .

Many extensions to theorem 1 exist, proving convergence of expanding functions in more general eigenfunctions than those of eq. (3.9). A notable extension is to the set of Regular Sturm-Liouville eigenvalue problems, outlined in chapter 5 of [10].

When a problem does not meet the requirements of these theorems, certain nice mathematical structures can not be taken for granted. For instance, for a general set of eigenfunctions  $\{\phi_n\}$ , it is not immediately clear which functions  $f$  are in the span of these eigenfunctions. In case  $f$  is in this span, eq. (2.3) can be generalised to

$$C_n = \frac{\langle f, \phi_n \rangle}{\langle \phi_n, \phi_n \rangle} \quad (2.5)$$

for a general inner product<sup>2</sup>, but only if the  $\{\phi_n\}$  are orthogonal under this inner product, meaning

$$\langle \phi_n, \phi_m \rangle = 0$$

---

<sup>2</sup>For the general definition of an inner product see for instance [12].



when  $n \neq m$ . In the case of a regular Sturm-Liouville problem, the problem itself provides a weight function  $\sigma(x) > 0$  to generalise the integral inner product with uniform weight used in section 3.1 to

$$\langle f, g \rangle := \int_0^L f(x)g(x)\sigma(x)dx, \quad (2.6)$$

an inner product under which the eigenfunctions are orthogonal automatically. In case no such inner product can be found, from any non-orthogonal (skew) bases an orthogonal basis can be constructed using the Gram-Schmidt procedure, see for instance Aliprantis et al. in chapter 6 of [12].

The question whether or not the basis following from an eigenvalue problem is orthogonal under a certain inner product can also be formulated in a different but equivalent way. We can reformulate eq. (3.7) as<sup>3</sup>

$$L\phi_n = -\lambda_n\phi_n \quad (2.7)$$

using a (linear) differential operator, in this case  $L := \frac{d^2}{dx^2}$ . We say that  $L$  is self-adjoint under a certain inner product if for that inner product the following holds for all  $n, m \in \mathbb{N}$ :

$$\langle L\phi_n, \phi_m \rangle = \langle \phi_n, L\phi_m \rangle. \quad (2.8)$$

It turns out that the basis  $\{\phi_n\}$  resulting from an eigenvalue problem is orthogonal under a certain inner product  $\langle \cdot, \cdot \rangle$  if the differential operator  $L$  that defines this eigenvalue problem is self-adjoint under the inner product  $\langle \cdot, \cdot \rangle$ .

One thing we do know for certain is that eigenfunctions belonging to different eigenvalues are linearly independent, which is a simple but important result from linear algebra.

## 2.4.2 The Fourier transform

We want to express the signal from the electric guitar in terms of the frequencies present in it. However, we do not know a priori which frequency oscillations are present in the signal, and at which (relative) amplitude. We therefore use a generalisation of the Fourier series called the Fourier transform, which expresses the signal in terms of a continuum of frequencies instead of a discrete set of frequencies. The Fourier transform calculates the weight function which expresses a function  $f$  on  $\mathbb{R}$  (which is possibly complex-valued) in terms of a continuous spectrum of frequencies over all real numbers:

$$C(\omega) = \frac{1}{2\pi} \int_{-\infty}^{\infty} f(x)e^{i\omega x} dx. \quad (2.9)$$

Analogous to theorem 1, this gives

$$\frac{1}{2}[f(x^+) + f(x^-)] = \int_{-\infty}^{\infty} C(\omega)e^{-i\omega x} d\omega. \quad (2.10)$$

Of the complex value  $C(\omega)$ , the modulus can be thought of as the amplitude, the same way as the absolute value of the  $C_n$  in eq. (2.2) can. The argument<sup>4</sup> of  $C(\omega)$  can be thought of as the phase shift corresponding to the frequency  $\omega$ . A big difference between the Fourier transform and the Fourier series is that the Fourier transform expresses a function on  $\mathbb{R}$  in terms of sines, whereas a Fourier sine series converges to the odd periodic extension of a function on a finite interval  $[0, L]$  with period  $L$ .

<sup>3</sup>Note that this notation also makes quite clear why  $\lambda_n$ , or strictly speaking  $-\lambda_n$ , is called an eigenvalue.

<sup>4</sup>This is angle in the complex plane between the line that connects a point in the complex plane to the origin and the positive real axis.

For the context of this text we are mainly interested in a numerical method which approximates  $C(\omega)$  for a given function  $f$ . In the context of this text,  $f$  will be the output signal of an electric guitar. The numerical method we use is called FFT (Fast Fourier Transform). The FFT approximates  $C(\omega)$  on a discrete set of equidistant points. The distance  $\Delta f$  between these points expressed as a frequency is determined by:

$$\Delta f = \frac{\text{sample rate}}{\text{number of samples}}. \quad (2.11)$$

We will call  $\Delta f$  the resolution. Here the sample rate is the number of measured samples per unit time. The number of points on which  $C(\omega)$  is approximated is  $\frac{1}{2} \times \text{number of samples} + 1$  (if the number of samples is even, which we will always make it to be) [6].



## Chapter 3

# The basic model for the electric guitar

In this chapter we describe the most basic model for the electric guitar based on the one-dimensional wave equation with homogeneous Dirichlet boundary conditions and a simple linear model for the pickup.

### 3.1 The simplest model for a string: the one dimensional ideal wave equation with Homogeneous Dirichlet boundary conditions

The aim of this section is to introduce the mathematical methodology for solving the one-dimensional wave equation with the most basic assumptions for modelling the motion of one string of an electric guitar. For an introduction into the subject from a physicist's point of view see Perov et al. in [7].

#### 3.1.1 The initial and boundary value problem

We describe the motion of the string of length  $L$  from bridge to nut using a function

$$u : [0, L] \times [0, \infty) \rightarrow \mathbb{R}, \quad (3.1)$$

where the first argument denotes the spatial coordinate  $x$  and the second argument the temporal coordinate  $t$ . The output denotes the displacement of the string from its equilibrium position, where we assume that the string only displaces vertically, that is, parallel to the fret board. We assume the string to be fixed at both ends:

$$u(0, t) = 0, \quad u(L, t) = 0, \quad \forall t \geq 0, \quad (3.2)$$

commonly known as homogeneous Dirichlet boundary conditions. Henceforth we denote the string in combination with its boundaries by 'the system'. We model the plucking of the string by giving it the initial displacement

$$u(x, 0) = \begin{cases} \frac{x}{x_{\text{pl}}} u_{\text{pl}} & \text{if } x \in [0, x_{\text{pl}}] \\ \frac{L-x}{L-x_{\text{pl}}} u_{\text{pl}} & \text{if } x \in (x_{\text{pl}}, L] \end{cases} \quad \forall x \in [0, L] \quad (3.3)$$

where  $x_{\text{pl}}$  is the horizontal position of the pluck on the string and  $u_{\text{pl}}$  the vertical displacement of the string at the point of the pluck. This initial condition can be seen in fig. 3.2 at  $t = 0$ .

As mentioned by Perov et al. in [7], in reality the initial shape of a guitar string is not perfectly triangular. This is due to the fact that the finger or plectrum the string is plucked with has a finite width. Furthermore, the bending stiffness of the string would prevent the string from assuming this shape, but it is assumed that the bending stiffness can be neglected in the derivation of the wave equation eq. (3.4). We assume the initial velocity of the string to be 0 at  $t = 0$  everywhere, so  $u_t(x, 0) = 0$  for all  $x \in [0, L]$ . For use of these initial conditions in further literature see for instance Fletcher in [9].

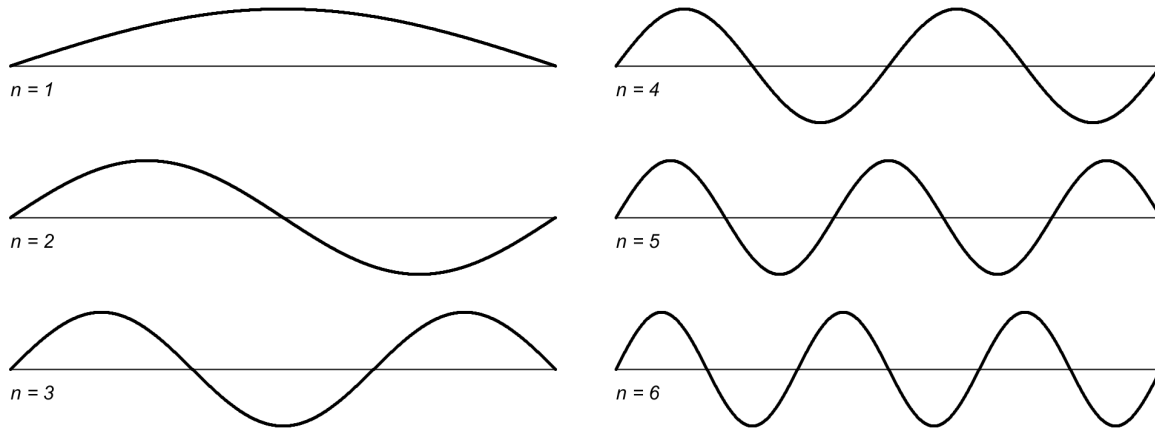


Figure 3.1: The first few modes of the string at  $t = 0$ . These modes are solutions to the damped wave equation (3.4) of the separated variable form  $\phi_n(x)\tau_n(t) \propto \sin(\frac{n\pi x}{L}) \sin(\omega_n t - \theta_n) e^{-\frac{\delta}{2}t}$ . The  $\phi_n$  form a basis for the function space described in theorem 1, of which the used initial conditions eq. (3.3) and  $u_t(x, 0) \equiv 0$  are also elements.

In this image and the following images of the string we look at the string from the same perspective as in fig. 2.1a, with the bridge at  $x = 0$  on the left and the nut at  $x = L$  on the right.

In this chapter, on the interior of the interval  $[0, L]$  and  $t > 0$  we assume the motion of the string to be governed by the one-dimensional wave equation<sup>1</sup>

$$u_{tt} + \delta u_t = c^2 u_{xx}, \quad (3.4)$$

The case  $\delta = 0$  is called the ideal wave equation and the case  $\delta > 0$  we call the damped wave equation. The parameter  $c$  depends on the tension on the string  $F_T$  and its linear density  $\mu$  by  $c^2 = \frac{F_T}{\mu}$ .  $\mu$  can be calculated from the diameter of the string  $d$  and the density of the string material  $\rho$  with the formula  $\mu = \frac{1}{4}\rho\pi d^2$ .  $c$  is often known as the ‘wave speed’, but we will see in section 3.1.3 to which extend that name can be justified in the context of eq. (3.4).

### 3.1.2 Solution by means of separation of variables

We solve this equation by looking for solutions with separated variables of the form  $\phi(x)\tau(t)$ , which we call normal modes.<sup>2</sup> The equation with separated variables is given by

$$\frac{1}{c^2} \frac{\ddot{\tau} + \delta\dot{\tau}}{\tau} = \frac{\phi''}{\phi} = -\lambda, \quad (3.5)$$

where we denote a spatial derivative by a prime and a temporal derivative by a dot. The minus sign on the right hand side is included to simplify the calculations later on. The method of separation of variables results in a general solution in the form of a superposition of all countably infinite eigenmodes<sup>3</sup>:

$$u(x, t) = \sum_{n=1}^{\infty} C_n \phi_n(x) \tau_n(t). \quad (3.6)$$

<sup>1</sup>For a derivation of the ideal one-dimensional wave equation see chapter 4 of [10].

<sup>2</sup>It is assumed that the reader is familiar with the process of solving by means of separation of variables. For an introduction into this method see chapter 2 of [10].

<sup>3</sup>The equals sign in eq. (3.6) at  $t = 0$  is validated by theorem 1.

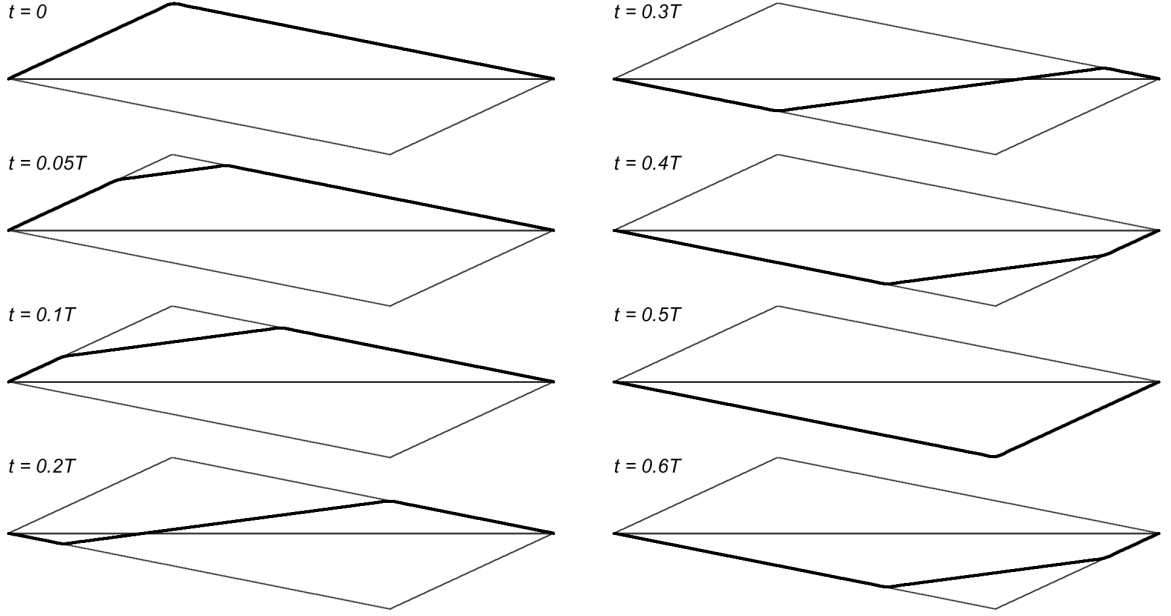


Figure 3.2: The position of the string in the case that  $\delta = 4\text{ s}^{-1}$  at various stages of a period  $T = \frac{1}{f_1}$ , where  $f_1$  is the ground frequency of the string. At this time scale the damping is not yet visible, as becomes clear from the figure at  $t = 0.5T$ .

For all  $n \in \mathbb{N}$ ,  $\phi_n$  is the solution to the problem

$$\phi_n'' + \lambda_n \phi_n = 0, \quad (3.7)$$

with boundary conditions

$$\phi_n(0) = \phi_n(L) = 0. \quad (3.8)$$

Eqs. (3.7) and (3.8) together we call the eigenvalue problem. This problem has the solutions

$$\phi_n(x) = \sin\left(\sqrt{\lambda_n}x\right) = \sin\left(\frac{n\pi x}{L}\right), \quad \lambda_n = \left(\frac{n\pi}{L}\right)^2. \quad (3.9)$$

For all  $n \in \mathbb{N}$ ,  $\tau_n$  is given by the problem

$$\ddot{\tau}_n + \delta \dot{\tau}_n + \lambda_n c^2 \tau_n = 0, \quad (3.10)$$

which has the solutions

$$\tau_n(t) = \sqrt{\frac{\delta^2}{4\omega_n^2} + 1} \cdot \sin(2\pi f_n t - \theta_n) e^{-\frac{\delta}{2}t} \quad (3.11)$$

$$2\pi f_n = \omega_n = \sqrt{\lambda_n c^2 - \left(\frac{\delta}{2}\right)^2} = \sqrt{\left(\frac{n\pi c}{L}\right)^2 - \left(\frac{\delta}{2}\right)^2} \quad (3.12)$$

$$\theta_n = \arctan\left(-\frac{2\omega_n}{\delta}\right), \quad (3.13)$$

already taking the initial condition  $u_t(x, 0) \equiv 0$  into account. Here  $f_n$  is the frequency of the  $n$ -th mode and  $\theta_n$  is its (temporal) phase shift.

The factor  $\sqrt{\frac{\delta^2}{4\omega_n^2} + 1}$  in  $\tau_n$  is inserted so that  $\tau_n(0) = 1$ . In fig. 3.1 we see the first few modes of the string. As mentioned by Perov et al. in [7], in physics terms these modes are

called transverse resonant standing waves. These modes are often characterised by the numbers of zeros (in this context often called nodes) these modes have, since as can be seen in fig. 3.1,  $n$  is equal to the amount of zeros of  $\phi_n(x)$  minus one.

The Fourier coefficients in eq. (3.6) are given by

$$C_n = \frac{L^2}{n^2\pi^2} \frac{2u_{\text{pl}}}{x_{\text{pl}}(L - x_{\text{pl}})} \sin\left(\frac{n\pi x_{\text{pl}}}{L}\right), \quad (3.14)$$

obtained using the integral inner product with uniform weight:

$$\langle f, g \rangle := \int_0^L f(x)g(x)dx, \quad (3.15)$$

making use of the orthogonality of the  $\phi_n$  under this inner product. For an elaborate derivation of eq. (3.14) see section 2.4 and Perov et al. in [7]. The position of the string in various stages of one ‘period’  $T = \frac{1}{f_1}$  is shown in fig. 3.2. See section 3.1.3 for an analysis of the periodicity of this solution.

### 3.1.3 Properties of the solution to the initial and boundary value problem

Equation (3.12) in combination with  $c^2 = \frac{F_T}{\mu}$  shows the relationship between the parameters  $F_T$ ,  $\mu$  and  $L$  and the frequencies present in the solution  $u$ . For the case  $\delta = 0$  these relationships are simply proportional to  $\sqrt{F_T}$ ,  $\frac{1}{\sqrt{\mu}}$  and  $\frac{1}{L}$  respectively. This agrees with the observations that a guitar string produces a higher pitched sound when the tension on it is increased, and that denser and/or thicker strings produce lower pitched sounds than less dense and/or thinner strings. The dependency on the string length of the pitch produced by a string is most noticeably exploited in grand piano’s, where each note is played using a separate string.

Using some trigonometric identities, a mode can be rewritten in the following way:

$$\phi_n(x)\tau_n(t) = \sin\left(\sqrt{\lambda_n}x\right) \sin(\omega_n t - \theta_n) e^{-\frac{\delta}{2}t} \quad (3.16)$$

$$= \frac{1}{2} \left[ \cos\left(\sqrt{\lambda_n}x - \omega_n t + \theta_n\right) - \cos\left(\sqrt{\lambda_n}x + \omega_n t - \theta_n\right) \right] e^{-\frac{\delta}{2}t}. \quad (3.17)$$

If we take a closer look at the arguments of the cosines in eq. (3.17) in combination with the equation for the angular frequencies of the modes eq. (3.12), we see that only in the case of the ideal wave equation, so  $\delta = 0$ , we can rewrite these arguments as  $\sqrt{\lambda_n}(x - ct)$  and  $\sqrt{\lambda_n}(x + ct)$  respectively (since in that case  $\theta_n = 0$ ). This means that only for the ideal wave equation we can rewrite the solution as  $u(x, t) = R(x - ct) + S(x + ct)$ , where  $R(x - ct)$  and  $S(x + ct)$  can be interpreted as waves moving respectively to the right and to the left with velocity  $c$ . In fact, the solution to the ideal wave equation with homogeneous Dirichlet boundary conditions can always be written in this form.<sup>4</sup> This is known as d’Alamberts solution, see chapter 12 section 5 of [10]. d’Alamberts solution does not require separation of variables and is therefore a faster solution method, but it does not provide the frequency spectrum we are interested in.

We have to be clear about what we mean by the period  $T = \frac{1}{f_1}$  mentioned earlier in this chapter. The solution eq. (3.6) is not periodic in the sense that  $u(x, t + kT) = u(x, t)$  for all  $x \in [0, L]$  and  $k \in \mathbb{Z}$  because of the damping term  $\delta$ . But even the validity of the equation  $u(x, t + kT) = u(x, t)e^{-\frac{\delta}{2}kT}$ , which seems to take the loss of amplitude due to damping into account, is not directly clear from equation eq. (3.12). Only when  $\delta = 0$  can we easily show that

<sup>4</sup>The solution does also contain an integral term with boundaries  $x - ct$  and  $x + ct$  when the initial velocity is not zero everywhere.

$T$  is the period of this solution in the sense of  $u(x, t + kT) = u(x, t)$ , because in that case  $T$  is the least common multiple of the periods of the modes, which in that case have period  $T_n = \frac{1}{nf_1}$ .

From plotting the solution for  $\delta > 0$  it does seem the case that  $u(x, t + kT) = u(x, t)e^{-\frac{\delta}{2}kT}$  holds, but if this equation holds, the proof is probably a bit less trivial than the  $\delta = 0$  case.

When in eq. (3.12) we choose  $c$  such that  $f_1$  becomes the desired frequency from table 2.1 and we substitute  $\lambda_n = \frac{n^2\pi^2}{L^2}$ , i.e.

$$c = L\sqrt{4f_1^2 + \left(\frac{\delta}{4\pi}\right)^2}, \quad (3.18)$$

we obtain the following insightful relation for the eigenfrequencies:

$$f_n = nf_1\sqrt{1 + \left(1 - \frac{1}{n^2}\right)\left(\frac{\delta}{4\pi f_1}\right)^2}. \quad (3.19)$$

From the exponential factor in eq. (3.11) we expect that  $u(x, t) \rightarrow 0$  for  $t \rightarrow \infty$  for all  $x \in [0, L]$  in the case that  $\delta > 0$ .<sup>5</sup> We can see that this is indeed the case by finding an upper bound for the absolute value of  $u(x, t)$ :

$$|u(x, t)| \leq \sum_{n=1}^{\infty} |C_n \phi_n(x) \tau_n(t)| \leq e^{-\frac{\delta}{2}t} \frac{L^2}{\pi^2} \frac{2u_{\text{pl}}}{x_{\text{pl}}(L - x_{\text{pl}})} \sqrt{\frac{\delta^2}{4\omega_1^2} + 1} \sum_{n=1}^{\infty} \frac{1}{n^2} \rightarrow 0 \quad (3.20)$$

as  $t \rightarrow \infty$  for all  $x \in [0, L]$ . Here we have used that  $(\omega_n)_{n \geq 1}$  is an increasing sequence and  $\sum_{n=1}^{\infty} \frac{1}{n^2}$  is a convergent series (which equals  $\frac{\pi^2}{6}$ ). From this it directly follows that  $u(x, t) \rightarrow 0$  for  $t \rightarrow \infty$  for all  $x \in [0, L]$  since  $e^{-\frac{\delta}{2}t}$  goes to 0 for  $t \rightarrow \infty$  and the factor  $\frac{2u_{\text{pl}}}{x_{\text{pl}}(L - x_{\text{pl}})} \sqrt{\frac{\delta^2}{4\omega_1^2} + 1}$  is finite and independent of  $n$ . Note that this result can also be obtained more directly from the initial and boundary value problem if we assume we know the solution converges to a steady state. In this steady state all partial derivatives of  $u$  with respect to time are identically zero, so eq. (3.4) reduces to  $u_{xx} = 0$ . This means that  $\lim_{t \rightarrow \infty} u(x, t)$  is linear in  $x$ . The only linear function that satisfies the homogeneous Dirichlet boundary condition is the function that is identically zero, so  $\lim_{t \rightarrow \infty} u(x, t) \equiv 0$ .

## 3.2 The pickup

As mentioned in section 2.3.2, we model the signal produced by the pickup as proportional to the speed of the string above the pickup. If we call the distance from the bridge to the pickup  $x_{\text{pu}}$ , we can define

$$S(t) := S_0 u_t(x_{\text{pu}}, t) = e^{-\frac{\delta}{2}t} \sum_{n=1}^{\infty} A_n \sin(2\pi f_n t). \quad (3.21)$$

as the prediction of the guitar output signal for some real proportionality constant  $S_0$ . We obtain the  $A_n$  by term-wise differentiating<sup>6</sup> eq. (3.6) using eqs. (3.11) and (3.12). This gives

$$A_n = S_0 C_n \phi_n(x_{\text{pu}}) \frac{\omega_n^2 + \left(\frac{\delta}{2}\right)^2}{\omega_n}. \quad (3.22)$$

<sup>5</sup>The case of the ideal wave equation  $\delta = 0$  gives a periodic solution, so in that case  $u$  does not converge for  $t \rightarrow \infty$ .

<sup>6</sup>See chapter 3 section 4 of [10] for an overview of in which cases term-wise differentiation of Fourier series is allowed.



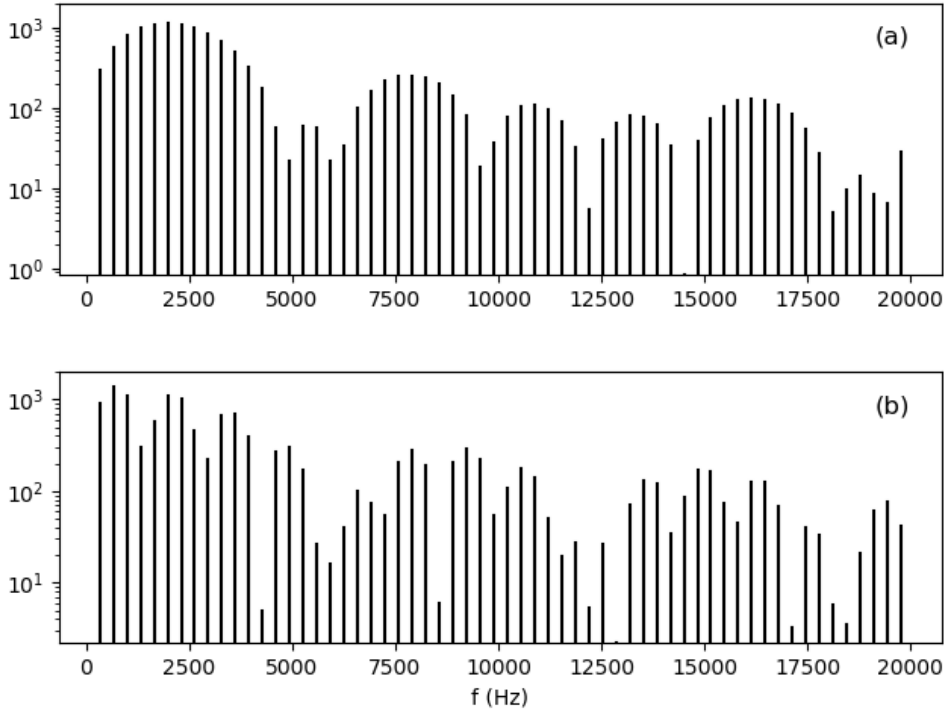


Figure 3.3: The predicted spectrum as a result of eq. (3.24). The used parameter values are:  $f_1$  is the ground frequency of the high E string from table 2.1,  $L = 0.645$  m,  $\delta = 4 \text{ s}^{-1}$ ,  $x_{\text{pl}} = 0.035$  m,  $S_0 = 1$ ,  $x_{\text{pu}} = 0.044$  m (a) and  $x_{\text{pu}} = 0.149$  m (b).

In the case of the model above this can be simplified to

$$A_n = S_0 \frac{c^2}{\omega_n} \frac{2u_{\text{pl}}}{x_{\text{pl}}(L - x_{\text{pl}})} \sin\left(\frac{n\pi x_{\text{pl}}}{L}\right) \sin\left(\frac{n\pi x_{\text{pu}}}{L}\right) \quad (3.23)$$

$$= S_0 \frac{c^2}{\omega_n} \frac{u_{\text{pl}}}{x_{\text{pl}}(L - x_{\text{pl}})} \left[ \cos\left(\frac{n\pi(x_{\text{pl}} - x_{\text{pu}})}{L}\right) - \cos\left(\frac{n\pi(x_{\text{pl}} + x_{\text{pu}})}{L}\right) \right]. \quad (3.24)$$

Equation eq. (3.22) also gives a predicted spectrum for the guitar output signal, with frequencies  $f_n$  and amplitudes  $A_n$ . For examples of such predicted spectra see fig. 3.3. fig. 3.3(a) shows the spectrum for a pickup at  $x_{\text{pu}} = 0.044$  m and fig. 3.3(b) shows the spectrum for a pickup at  $x_{\text{pu}} = 0.149$  m. The difference between these spectra agrees with the experience from electric guitarists that pickups closer to the bridge produce a sharper sound than pickups further away from the bridge. fig. 3.3(a) shows an overall fuller spectrum with larger amplitudes of the frequencies towards the high end of the frequencies present in the signal within hearing range.

Equations (3.18) and (3.19) tell us that when we assume the guitar is tuned perfectly, i.e. such that the ground frequency of a string corresponds with the ground frequency from table 2.1,  $c^2$  is proportional to  $L^2$  and  $\omega_n$  does not depend on  $L$ . This tells us that eq. (3.24) can be rewritten purely in terms of the relative pluck and pickup positions  $\frac{x_{\text{pl}}}{L}$  and  $\frac{x_{\text{pu}}}{L}$  in stead of the absolute pickup positions  $x_{\text{pl}}$  and  $x_{\text{pu}}$  and the string length  $L$  independently. In other words: this model predicts that the spectrum of the signal produced by the guitar only depends on the relative positions of the pluck and the pickup, not on their absolute position. This means that scaling the string and the pluck and pickup positions equally does not affect the signal produced by the electric guitar.

### 3.3 Reflection on the assumptions made to obtain this model

In the construction of the model above, a lot of simplifying assumptions were made, so here we give an overview of some of them. First we look at the assumptions made in formulating the initial and boundary value problem:

- We assume each point of the string has one degree of freedom moving in one dimension parallel to the fret board of the guitar.
- We assume that the displacement of the string at the string boundaries is zero at all times and so there is no transport of energy from the string to the guitar body through the string boundaries.
- We assume that the velocity of all points on the string at the instant of plucking it is zero.
- We assume that the bending stiffness of the string is negligible.
- We assume that the width of the finger or plectrum that the string is picked with is negligible.
- We assume that the damping the string experiences is directly proportional to the velocity of the string. Usually air resistance is modelled proportional to the square of the velocity of an object, but that would make eq. (3.4) nonlinear which would make it much harder to solve.
- We assume the linear density  $\mu$  of the string is uniform.
- We assume the tension  $F_T$  on the string is constant in time and space, independently of the motion of the string.
- We assume that the approximations that were made in the derivation of the wave equation are valid. This involves approximations like the small angle approximation  $\sin(\theta) \approx \tan(\theta) = \frac{\partial u}{\partial x}$  are valid.<sup>1</sup>

Now we look at the assumptions made in the model for the pickup:

- We assume that the signal produced by the pickup depends linearly on the string velocity.
- We assume that the signal produced by the pickup only depends on the velocity  $u_t(x_{pl}, t)$  of the point on the string directly above the pickup.
- We assume each coil in the pickup only detects the influence of the string directly above it.

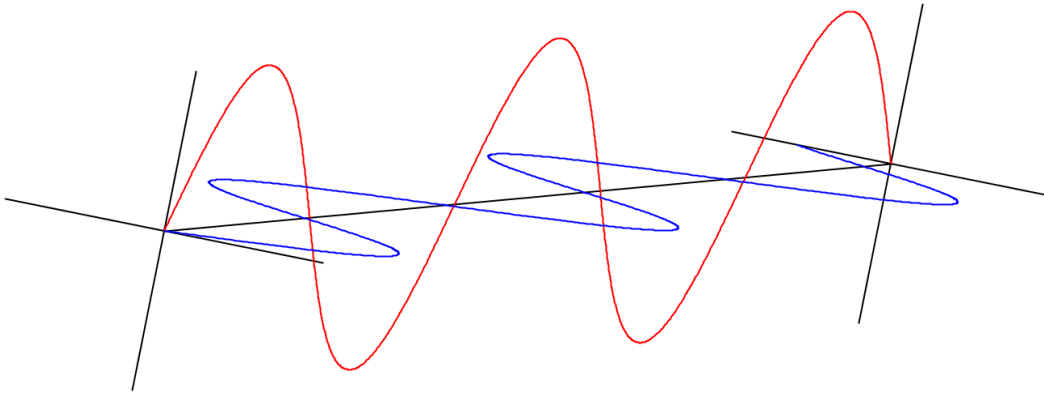


Figure 3.4: Modes parallel (red) and perpendicular (blue) to the fret board, differing slightly in spatial (and temporal) frequency. These differences are caused by slightly different interactions of the string with the rest of the guitar for parallel and perpendicular modes. We assume the string to be in a superposition of parallel and perpendicular modes.

### 3.4 Parallel and perpendicular modes

In the model of the motion of the string described in section 3.1 we assumed that the string only moves in the direction parallel to the fret board. The string is however also free to move in the direction perpendicular to the fret board. Instead of solving the wave equation eq. (3.4) with an additional spatial degree of freedom, we think of the string as having parallel and perpendicular modes, and the position of the string as a superposition of these modes. According to Fletcher et al. in section 5.6 of [2], non-linear effects in the string causes exchange of energy between the parallel and perpendicular modes. This means that even if the string is plucked perfectly parallel to the fret board, the perpendicular modes also get excited eventually.

The perpendicular and parallel modes do not necessarily behave exactly the same way. In fact, they can have different effective values of certain parameters, like  $\delta$  (and also  $m_0$ ,  $m_L$ ,  $\omega_{b0}$  and  $\omega_{bL}$  which will be introduced in chapter 5). These differences can for instance be caused by the difference in interaction of the string with the bridge and nut between parallel and perpendicular modes. These differences cause the parallel and perpendicular modes with the same  $n$  to have slightly different temporal and (in the case of the oscillating boundaries in chapter 5) spatial frequencies, see fig. 3.4.

In as far as the pickup detects both types of mode in a similar way, we can see what the effect is of detecting the parallel and perpendicular modes with (almost) the same number of nodes when they have a very slight difference in frequency  $2\Delta f$ :

$$\begin{aligned}
 & A \sin(2\pi[f_0 - \Delta f]t) + B \sin(2\pi[f_0 + \Delta f]t) \\
 = & (A + B) \sin(2\pi f_0 t) \cos(2\pi \Delta f t) + (A - B) \cos(2\pi f_0 t) \sin(2\pi \Delta f t). \quad (3.25)
 \end{aligned}$$

The effect that we see is called beating, caused by the modes getting slowly in and out of phase due to their slight difference in frequency. Beating is a low frequency modulation of the amplitude. The factors  $\cos(2\pi \Delta f t)$  and  $\sin(2\pi \Delta f t)$  determine the envelope. More on the envelope and beating can be read in section 4.3.

## Chapter 4

# Comparing the basic model to measurements

### 4.1 Obtaining parameter values for the Fender Lead III

Now that we have a model for the string and the pickup of an electric guitar, we need to find values for the parameters in this model in order to compare the predictions of this model to real world measurements. The guitar used in all the measurements for this text is a Fender lead III, built in 1982.

Some parameter values are really easy to measure, like the string length  $L = 645$  mm from the bridge to the nut. There is however a slight complication with the measurement of the pickup positions. The Fender lead used for the experiments has 2 Humbucker pickups, which were only used in single coil mode. It is not clear which of the two rows of coils in each Humbucker pickup gets used in the single coil mode. In the calculations in this chapter we assume that the coil the furthest from the bridge was used. The distances from the bridge to the center of the 2 Humbucker pickups, henceforth denoted by pickup 1 and pickup 2, are 35 mm and 140 mm respectively. The distance between both rows of coils of a single Humbucker pickup is 18 mm.

The value of the damping parameter  $\delta$  can be obtained from fits of the output signal of the guitar, see section 4.3.2.

### 4.2 Experimental setup

The circumstances of these measurements and the equipment used are:

- The guitar is connected to a linear mixing desk directly, no guitar amplifier was used. All knobs of the track (filters) are set to neutral.
- The recording is done with the digital audio workstation Ardour, with a Juli@ soundcard on a Linux PC. The signal of the guitar is saved as an uncompressed WAVE file on 1 channel, with a sample width of 3 and a frame rate of 96 kHz.<sup>1</sup>
- The guitar is tuned using an electronic tuner.
- The temperature in the room during the measurements is about 12 °C.

The following measurements were repeated for the high-E, the B and the G string:

- Using pickup 1, pluck the string by hand with a plastic plectrum first at  $x_{\text{pu1}}$ , then after a few seconds at  $x_{\text{pu2}}$ , then after a few seconds at  $L/2$ .<sup>2</sup>
- repeat the measurements above using pickup 2.

---

<sup>1</sup>For more details on WAV files see appendix B.

<sup>2</sup>The middle of the string  $L/2$  is not hard to find since there is a fret there. This fret is usually used to play the note one octave above the note corresponding to the open string.

This gives us a total of  $3 \times (3+3) = 18$  measurements. The duration between two plucks is about 8-10 seconds, and the force with which the strings are plucked is not tightly controlled, but an effort was made to make the force of all plucks as similar as possible.

### 4.3 Properties of the wave forms

#### 4.3.1 Qualitative properties of the wave forms: the envelope, decay and beating

In appendix A, Images A.1, A.2 and A.3 show the wave forms of the measurements mentioned in the previous section. In fig. A.4 the measurement of the high E string plucked at  $x_{\text{pu1}}$  using pickup 1 is shown again, but here at various time scales.

Since we want to discuss the overall shape of these wave forms, we introduce the concept of the upper and lower envelope: functions that outline the extremes of the signal. More specifically: we define the upper and lower envelope as the functions that respectively connect the maxima and minima in each ‘period’  $T = \frac{1}{f_1}$ . Again we have to be careful with the term period here, since fig. A.4 shows that the signal is not periodic in any nontrivial way. We will denote the upper and lower envelopes together by ‘the envelope’.

The measurements show that indeed the signal decays over time, as predicted in section 3.1. This shows that the damping term in eq. (3.4) is a valuable extension of the wave equation for describing the signal of the electric guitar. See section 4.3.2 how we obtain some estimations for the value of the parameter  $\delta$ .

The measurements also contain beating. As explained in section 3.4, we suspect this beating to be caused by parallel and perpendicular modes getting in and out of phase with each other because they have slightly different temporal frequencies. The measurements do not all show the same beating pattern and in some measurements the beating is more clear than in others. Since the measurements weren’t very controlled, it is hard to say based on these measurements alone which factors of the electric guitar affect the beating frequency. In general the measurements with pickup 1 show a larger beating frequency than the measurements with pickup 2. A possible explanation for this is that there is a difference between the pickups in how strong each mode gets detected (see section 3.2). This means that which mode numbers difference between the parallel and perpendicular modes frequency dominates the beating of the signal is dependent on the pickup position.

We use the estimations of the parameter  $\delta$  in section 4.3.2 to see if it is likely that the difference in temporal frequencies of the parallel and perpendicular modes is caused by them having different effective values of  $\delta$ .

#### 4.3.2 Quantitative properties of the wave forms: fitting the damping parameter and comparing the measurements to the predicted waveform

To get an idea of the order of magnitude of the parameter  $\delta$ , we fit the function  $Ae^{-\frac{\delta}{2}(t-t_0)}$  to the upper and lower envelopes of the signal. We use this exponential function because it shows up in eq. (3.11) and is independent of the mode so it can be factored out of the sum in eq. (3.6).  $t_0$  is the time at which the signal reaches its global maximum (for the upper envelope) or global minimum (for the lower envelope). These fits were performed with the function `curve_fit` from the library python library `scipy.optimize`.<sup>3</sup> The results of this are shown in table 4.1, and an example of the fits can be seen in fig. 4.1.

<sup>3</sup>See <https://docs.scipy.org/doc/scipy/reference/optimize.html>.

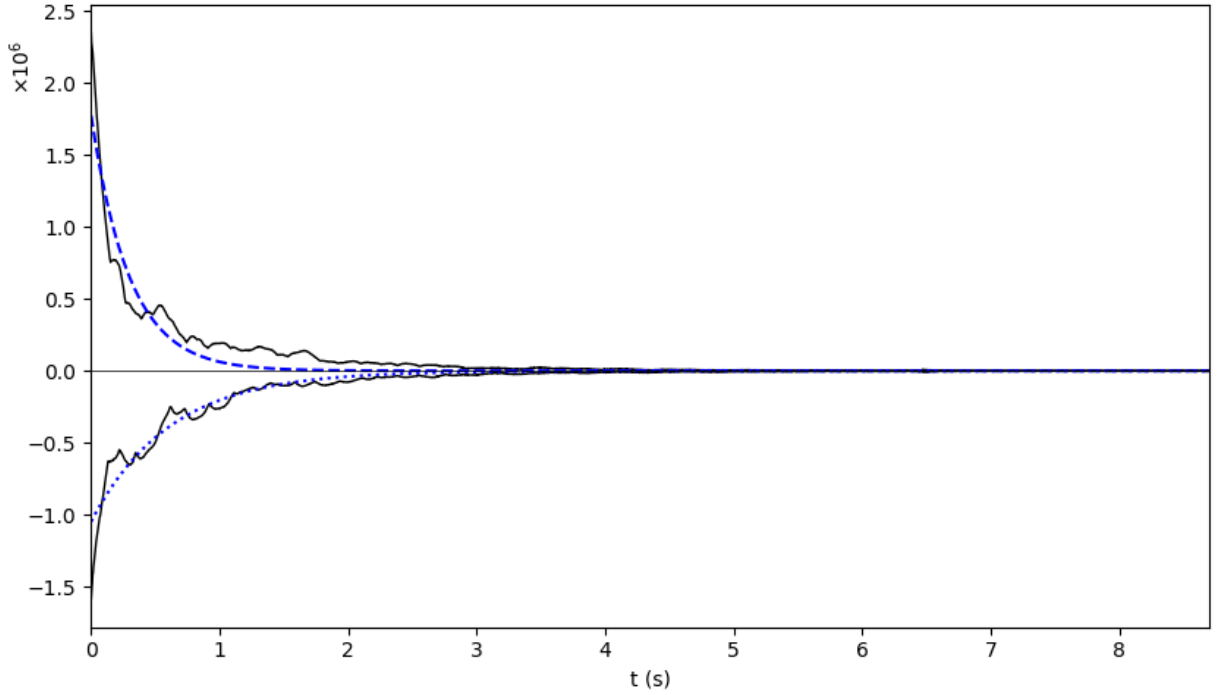


Figure 4.1: Fits (blue) of the function  $Ae^{-\frac{\delta}{2}(t-t_0)}$  to the upper and lower envelopes (black) of the signal, in this case a measurement of the high E-string plucked at pickup 1 measured with pickup 1. The upper and lower envelopes are obtained by respectively connecting the maxima and the minima in each ‘period’ of length  $T = \frac{1}{f_1}$ , starting at  $t = t_0$ .  $t_0$  is the time at which the signal reaches its global maximum (for the upper envelope) or global minimum (for the lower envelope).

Table 4.1: Values of  $\delta$  obtained by fitting  $Ae^{-\frac{\delta}{2}(t-t_0)}$  to the upper and lower envelopes.  $t_0$  is the time at which respectively the global maximum and minimum value of the signal occurs. The envelopes are obtained by connecting respectively the maxima and the minima of the signal in each ‘period’  $T = \frac{1}{f_1}$ , starting at  $t = t_0$ .

(a) Values of  $\delta$  (in  $s^{-1}$ ) obtained by fitting  $Ae^{-\frac{\delta}{2}(t-t_0)}$  to the upper envelope.

string name	$x_{pl}$	pickup 1	pickup 2
high E	$x_{pu1}$	6.705	3.258
	$x_{pu2}$	3.154	3.066
	$L/2$	2.301	1.922
B	$x_{pu1}$	3.687	1.941
	$x_{pu2}$	2.232	1.921
	$L/2$	1.774	1.025
G	$x_{pu1}$	1.831	1.175
	$x_{pu2}$	1.442	1.166
	$L/2$	1.324	0.830

(b) Values of  $\delta$  (in  $s^{-1}$ ) obtained by fitting  $Ae^{-\frac{\delta}{2}(t-t_0)}$  to the lower envelope.

string name	$x_{pl}$	pickup 1	pickup 2
high E	$x_{pu1}$	3.308	3.233
	$x_{pu2}$	2.816	2.551
	$L/2$	2.175	1.793
B	$x_{pu1}$	2.324	2.145
	$x_{pu2}$	2.245	1.889
	$L/2$	2.033	1.106
G	$x_{pu1}$	1.727	1.053
	$x_{pu2}$	1.406	0.823
	$L/2$	1.384	0.825

In fig. 4.2 we see the prediction of the signal produced by plucking the high E string at pickup 1 using pickup 1, with  $\delta$  the average of the fitted deltas for the upper and lower envelope of the corresponding measurement from table 4.1. This prediction uses 1000 modes. Comparing this to

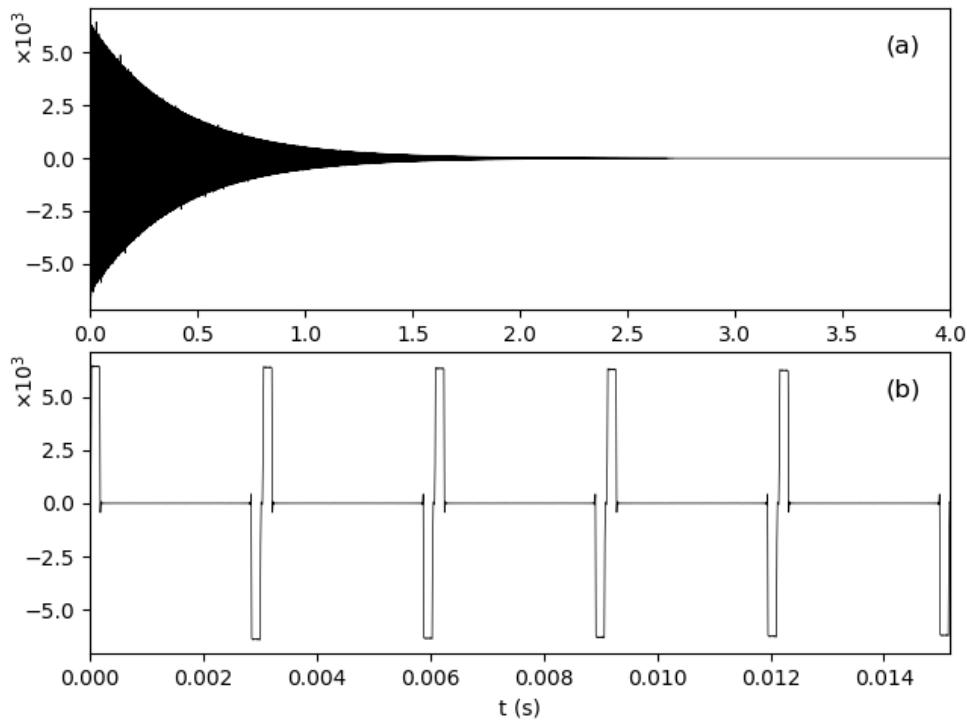


Figure 4.2: Prediction using 1000 modes of the signal produced by plucking the high E string at pickup 1 using pickup 1, with  $\delta$  the average of the fitted deltas for the upper and lower envelope of the corresponding measurement from table 4.1

fig. A.4 shows that the exponential damping roughly agrees with the damping in the measured signals. There is however a lot of complexity in the measured signals that is not captured by the current model. Some of that complexity might be due to the interaction between parallel and perpendicular modes, see section 3.4. It can also be caused by interactions between the string and the guitar body, see chapter 5. When we write this predicted signal to a WAV file and listen to it, it sounds more like an old fashioned ringtone than an electric guitar.

The irregularities around the tops and the bottoms of the peaks in fig. 4.2 are probably due to the Gibbs phenomenon, which says that Fourier series converge rather poorly (and non-uniformly) around jump discontinuities in the limit function or in the derivative of the limit function.

The shape of the signal in detail in figure fig. 4.2(b) can be understood by looking at fig. 3.2, which shows that the model predicts that certain sections of the string are stationary during certain parts of a ‘period’.

## 4.4 Properties of the spectra

### 4.4.1 Qualitative properties of the spectra

Figures A.5, A.6 and A.7 show the spectra of the measurements, obtained by applying the Fast Fourier Transform to the measured signals. Figure A.8 shows again the FFT of the signal produced by plucking the high E string plucked at  $x_{pu1}$  using pickup 1, but at various time scales. The amplitudes are plotted logarithmically in stead of lineary to bring out more detail, but also because of the logarithmic sensitivity of the human ear, see section 2.1.

These plots only show the modulus of the complex output of the FFT, which give the amplitudes corresponding to the frequencies in the domain. The information that is not shown is the phase shifts encoded in the arguments of the FFT output. As mentioned in section 2.1, the influence of the phase shifts on how we perceive sound is small compared to the influence of the amplitudes.

We denote measured frequencies with a tilde ( $\sim$ ). At first sight the spectrum looks fairly harmonic, meaning that all peaks in the spectrum are at an integer multiple of the ground frequency  $\tilde{f}_1$ , which is the ‘first large peak’ roughly at where we expect it based on table 2.1. Note that our model also predicts a harmonic spectrum for  $\delta = 0$ , see eq. (3.19). However, as is mentioned by Fletcher et al. in section 5.5 of [2], precisely harmonic systems do not exist. See section 4.4.2 for a quantification of how unharmonic the spectra are.

It is unclear how exactly the beating presents itself in the spectra. Following the reasoning presented in section 3.4 as an explanation for beating, we expect to find two peaks in the spectra whose difference is twice the frequency of the observed beating. We also expect these peaks to be among the highest in the spectrum, because only then they have a significant influence on the envelope of the guitar signal.

Investigation of the spectra showed that there is not very consistently a double peak with the desired difference in frequency we expect. Figure 3.4(c) does show a double peak, but given that the scale is logarithmic the smaller peak is so much smaller than the bigger peak that it is unlikely that this is the cause of beating. Figure 3.4(c) does show that the largest peak is quite broad, in the order of 1 Hz. This is consistently true for the other peaks in the spectra. This might be the cause of beating, but it would take a further investigation of Fourier transforms to give a definitive answer to this question, which we will not go into here. The broadness of these peaks could be caused by a different process than the interference of parallel and perpendicular modes.

#### 4.4.2 Quantitative properties of the spectra

To see how close the spectra are to being harmonic, we look for the peaks in the spectra  $\tilde{f}_n$  as the maxima in the intervals  $[(n - \frac{1}{2})f_1, (n + \frac{1}{2})f_1]$  with  $f_1$  from table 2.1. Then we calculate the relative deviation from the harmonic spectrum as a percentage using the equation

$$\Delta f_{\text{rel}}(n) = 100\% \cdot \frac{\tilde{f}_n - n\tilde{f}_1}{n\tilde{f}_1}. \quad (4.1)$$

The results of this calculation are shown in fig. 4.3. Since in section 2.1 it was mentioned that a difference in 0.03 % between frequencies is noticeable, the deviations from the harmonic spectrum shown in fig. 4.3 are certainly significant in the context of human hearing.

Now we take a closer look at eq. (3.19). Substituting eq. (3.19) in eq. (4.1) gives a predicted deviation of

$$\Delta f_{\text{rel}}(n) = 100\% \cdot \left[ \sqrt{1 + \left(1 - \frac{1}{n^2}\right) \left(\frac{\delta}{4\pi f_1}\right)^2} - 1 \right] < 100\% \cdot \left[ \sqrt{1 + \left(\frac{\delta}{4\pi f_1}\right)^2} - 1 \right]. \quad (4.2)$$

The first thing to notice is that eq. (4.2) only predicts positive deviations, while fig. 4.3 shows that the G and B strings also show negative deviations. What’s more, the predicted deviations with the values of  $\delta$  in table 4.1 are way too small when we compare them to fig. 4.3. If we take for each string the biggest value of  $\delta$  and calculate the upper bound given in eq. (4.2), we obtain  $1.310 \times 10^{-4}$  % for the high E string,  $7.058 \times 10^{-5}$  % for the B string and  $2.458 \times 10^{-5}$  % for the G string. As a rule of thumb, we say it is likely that an effect can cause the beating observed in



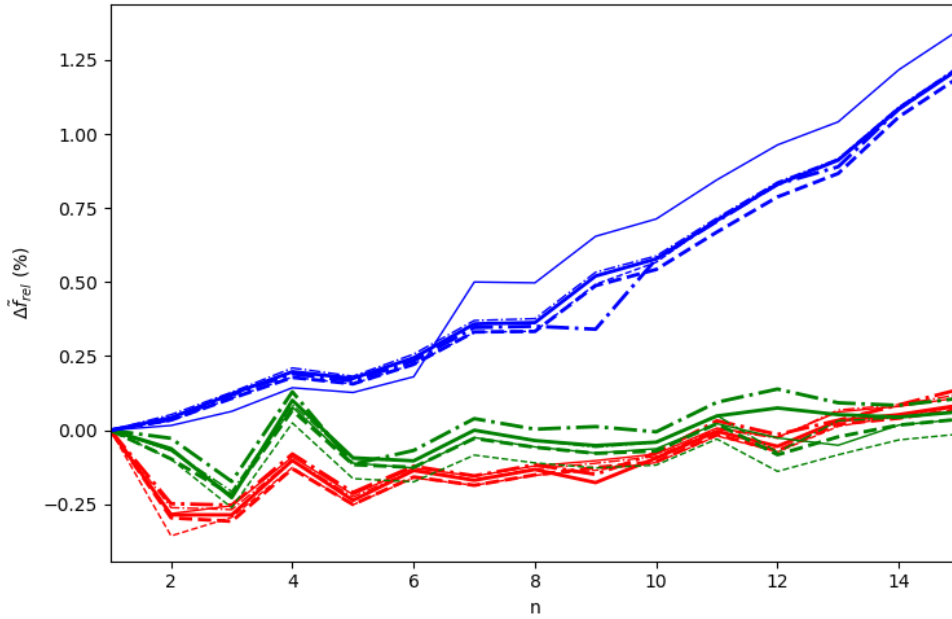


Figure 4.3: Relative deviation of the peaks at  $\tilde{f}_n$  in the measured spectrum from an harmonic spectrum given by  $nf_1$ , as a percentage. The peaks  $\tilde{f}_n$  are found as the maxima in the intervals  $[(n - \frac{1}{2})f_1, (n + \frac{1}{2})f_1]$ , where  $f_1$  is the expected ground frequency from table 2.1.

The colors indicate the string: Green for the high E string, red for the B string, blue for the G string. The non-bold lines indicate measurements with pickup 1, the bold lines indicate measurements with pickup 2. The linestyles indicate where the string is plucked: solid for  $x_{pu1}$ , alternating dots and dashes for  $x_{pu2}$ , dashed for  $L/2$ .

the measurements if it can cause deviations in the spectrum in the order of 1% of the frequency of the ground mode, which is not the case here.

This also means that  $\delta$  does not have the right order of magnitude to explain the beating. For instance, if for the high E string we assume the parallel modes to have an effective  $\delta$  of 6 and the perpendicular modes to have an effective delta of 3, the 1928<sup>th</sup> modes would be the first to have a frequency difference larger than 0.5 Hz. Not only is this far outside the auditory range, by eq. (3.24) we expect the amplitudes to be inversely proportional to their angular frequency, so we do not expect the 1928<sup>th</sup> mode to have a significant influence on the signal we can see as beating.

There is another way in which we can argue that the damping alone does not explain the deviation from a harmonic spectrum. We can namely try to fit eq. (3.19) to the  $\tilde{f}_n$ . An example of this is shown in fig. 4.4. Since by eq. (3.24) the signal is proportional to  $u_{pl}$  and  $S_0$  and we know neither of these constants, we scale the all the amplitudes by the same factor such that the amplitude of  $f_1$  matches the amplitude of  $\tilde{f}_1$  exactly. These fits produce very inconsistent results, with  $\delta$  ranging from almost 0 (which causes the prediction to damp way too slowly) to in the order of 100 (which causes the prediction to damp way to quickly). In fig. 4.4 it looks like at least for  $f_n < 5$  kHz the predicted amplitudes match the spectrum quite well, but it should be emphasized that this is not the case for all spectra.

Since we have concluded that the parameter  $\delta$  can not explain the deviation from harmonic spectra and beating, we need to introduce something new into the model. In the next chapter we therefore look at the influence of modelling the string boundaries as harmonic oscillators coupled to the string, as mentioned by Fletcher et al. in section 5.6 of [2].

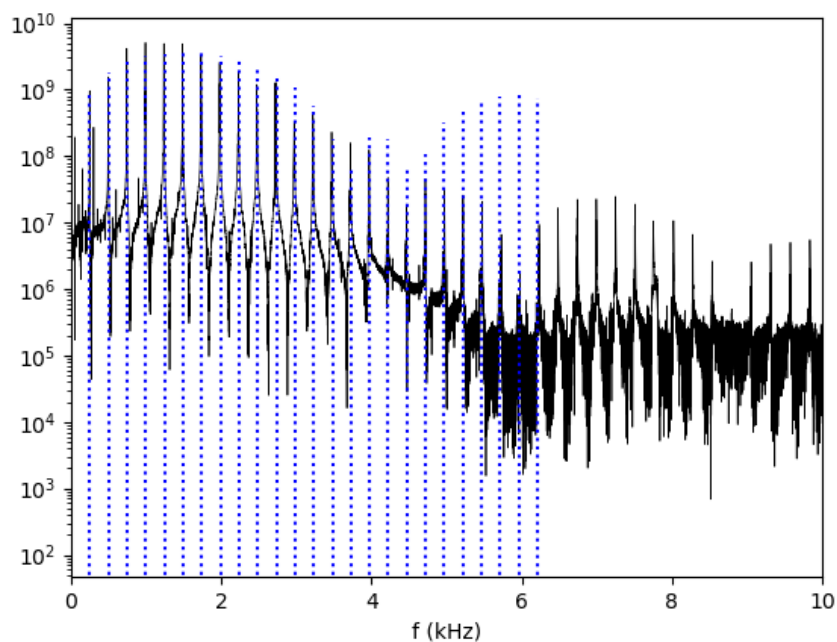


Figure 4.4: Fit of the spectrum of the pluck of the B string plucked at pickup 1 measured with pickup 1. The predicted spectrum is shown as the blue dotted lines. All the amplitudes in the spectrum are scaled with the same factor such that the measured amplitude of  $\tilde{f}_1$  matches the predicted amplitude of  $f_1$  exactly.



## Chapter 5

# String boundaries modelled by oscillators

Probably everyone who has ever played a guitar knows that when you play the guitar, the body starts to vibrate.<sup>1</sup> This means that somehow energy has to be transferred from the strings to the body of the guitar. One of the possible ways for this to happen is through the string boundaries, which we will look at here. We assume the string boundaries are free to oscillate, which is a relaxation of the homogeneous Dirichlet boundary conditions used in chapter 3.

It is also suggested by Fletcher et al. in section 5.6 of [2] that parallel and perpendicular modes couple to the bridge and nut differently, which may cause the beating observed in the measurements, as explained in section 3.4.

### 5.1 Boundary conditions

#### 5.1.1 Equation of motion for the boundaries

If we no longer assume the guitar string is fixed at both ends at all times, we need to formulate some rules that govern the behaviour of the boundaries. We know that the displacement of the string at the boundaries is so small that it is invisible to the naked eye. We therefore need some force that restores the boundaries to equilibrium, the simplest form of which is Hooke's law:

$$F_{H,0} = -\kappa_0 b_0(t), \quad F_{H,L} = -\kappa_L b_L(t), \quad (5.1)$$

for some real positive constants  $\kappa_0$  and  $\kappa_L$ . Here  $b_0(t)$  denotes the displacement of the left boundary and  $b_L(t)$  the displacement of the right boundary over time.

Of course the boundaries are also coupled to the interior of the string. This is done in terms of the tensile force:

$$F_{T,0} = F_T u_x(0, t), \quad F_{T,L} = -F_T u_x(L, t). \quad (5.2)$$

Notice the difference in sign between both boundaries. These expressions denote the component of the tensile force in the direction perpendicular to the equilibrium position of the string. The partial derivative is obtained using small angle approximations of the angle  $\beta(x, t)$  the string makes with the line parallel to the equilibrium position of the string:  $\sin(\beta(x, t)) \approx \tan(\beta(x, t)) = u_x(x, t)$ .

We also expect the boundaries to be damped:

$$F_{d,0} = -\delta m_0 \dot{b}_0(t), \quad F_{d,L} = -\delta m_L \dot{b}_L(t). \quad (5.3)$$

For this we use the same damping coefficient  $\delta$  as for the interior of the string in eq. (3.4), since using a different damping coefficient highly complicates if not forbids separation of variables

---

<sup>1</sup>This effect is much more prominent in acoustic guitars, but certainly also present in electric guitars.

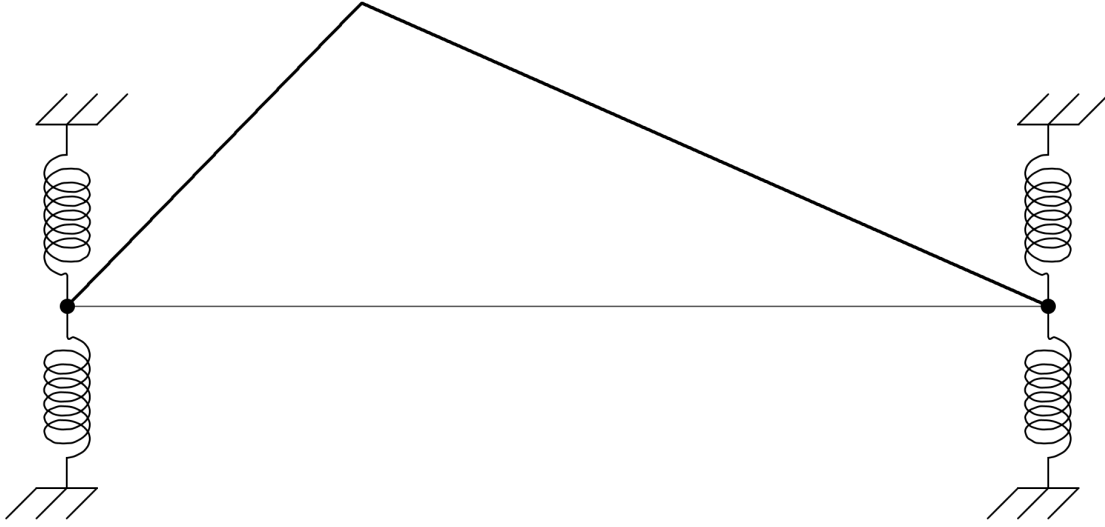


Figure 5.1: Schematic representation of the new boundary conditions. The black dots denote the masses  $m_0$  (left) and  $m_L$  (right). The springs denote the working of Hooke's law.

in the calculations that follow. Now we can use Newton's second law of motion combined with eqs. (5.1) to (5.3) to obtain

$$m_0 \ddot{b}_0(t) + \delta m_0 \dot{b}_0(t) + \kappa_0 b_0(t) = F_T u_x(0, t) \quad (5.4)$$

$$m_L \ddot{b}_L(t) + \delta m_L \dot{b}_L(t) + \kappa_L b_L(t) = -F_T u_x(L, t). \quad (5.5)$$

By eqs. (5.4) and (5.5)  $b_0$  and  $b_L$  describe the vertical positions of damped harmonic oscillators with an inhomogeneous forcing term which couples them to the string. Were these oscillators not forced (so the right hand side of these equations would be zero), these oscillators would show a behaviour very similar<sup>2</sup> to the modes described in section 3.1:

$$b(t) = A \sin \left( t \sqrt{\frac{\kappa}{m} - \left(\frac{\delta}{2}\right)^2} - \theta \right) e^{-\frac{\delta}{2}t}, \quad (5.6)$$

for certain constants  $A$  and  $\theta$  determined by initial conditions. We therefore write  $\omega_{b_0}^2 = \frac{\kappa_0}{m_0}$  and  $\omega_{b_L}^2 = \frac{\kappa_L}{m_L}$  for the angular frequencies with which  $b_0$  and  $b_L$  would oscillate if they were not coupled to the string and undamped.

However, this viewpoint can be misleading since certainly  $u$  is not independent from  $b_0$  and  $b_L$ . In fact, we say that  $b_0(t) \equiv u(0, t)$  and  $b_L(t) \equiv u(L, t)$  because the string is attached to the vibrating masses at  $x = 0$  and  $x = L$ . This gives

$$m_0 u_{tt}(0, t) = F_T u_x(0, t) - \kappa_0 u(0, t) - \delta m_0 u_t(0, t) \quad (5.7)$$

$$m_L u_{tt}(L, t) = -F_T u_x(L, t) - \kappa_L u(L, t) - \delta m_L u_t(L, t). \quad (5.8)$$

These boundary conditions are a very rudimentary model of the expected interaction between the string and the guitar body on the left side, and the string and the fret board on the right

<sup>2</sup>Unless  $(\frac{\delta}{2})^2 \geq \frac{\kappa}{m}$ , in which case the amplitude of  $b$  would decrease exponentially without oscillating. The same holds true for modes in section 3.1 for which  $(\frac{\delta}{2})^2 \geq \lambda_n c^2$ . Those solutions are not present if  $c$  is sufficiently large so they are probably not relevant given the high tension on the strings of an electric guitar.

side of the guitar. It should therefore be emphasized that the values  $m_0$ ,  $m_L$ ,  $\omega_0$  and  $\omega_L$  do not correspond to direct measurements of the guitar, like the way for instance the string length  $L$  does. These parameters should be given ‘effective’ values, for which the predictions of this model most closely resemble the measurements of a real electric guitar.

### 5.1.2 Separation of variables

Since we did not change the PDE used in section 3.1 (that is, eq. (3.4)), we shall again look for separable solutions  $\phi(x)\tau(t)$ . These still satisfy

$$\frac{1}{c^2} \frac{\ddot{\tau} + \delta\dot{\tau}}{\tau} = \frac{\phi''}{\phi} = -k^2. \quad (5.9)$$

Anticipating the result eq. (5.10), we write the constant of separation in terms of the wave number  $k$  here. The harmonic solution for  $\phi(x)$  of eq. (5.9) is

$$\phi(x; k) = A(k) \cos(kx) + B(k) \sin(kx) \quad (5.10)$$

for the  $x$  dependent problem, and

$$k^2 \leq \frac{\delta^2}{4c^2} : \quad \tau(t; k) = [C(k)e^{\beta(k)t} + D(k)e^{-\beta(k)t}] e^{-\frac{\delta}{2}t} \quad (5.11)$$

$$k^2 > \frac{\delta^2}{4c^2} : \quad \tau(t; k) = [C(k) \cos(\omega(k)t) + D(k) \sin(\omega(k)t)] e^{-\frac{\delta}{2}t} \quad (5.12)$$

for the  $t$  dependent problem, where

$$\omega(k) = \sqrt{k^2c^2 - \left(\frac{\delta}{2}\right)^2} \in \mathbb{R} \quad (5.13)$$

$$\beta(k) = \sqrt{\left(\frac{\delta}{2}\right)^2 - k^2c^2} \in \mathbb{R}, \quad (5.14)$$

in the respective intervals for  $k$  in eqs. (5.13) and (5.14). We discard the solutions for  $k^2 \leq \frac{\delta^2}{4c^2}$ , since those do not produce oscillations that contribute to the spectrum.

Note that the boundary conditions for  $u$ , eqs. (5.7) and (5.8), are linear and homogeneous. This means that if we look for solutions  $\phi_n(x; k)\tau(t; k)$  that satisfy these boundary conditions, any superposition of these solutions also satisfies these boundary conditions (and also the PDE eq. (3.4) because of its linearity).<sup>3</sup> Substituting  $\phi_n(x; k)\tau(t; k)$  in eq. (5.7) and eq. (5.8) gives

$$0 = m_0A(k)\ddot{\tau}(t; k) - F_TkB(k)\tau(t; k) + \kappa_0A(k)\tau(t; k) + \delta m_0A(k)\dot{\tau}(t; k) \quad (5.15)$$

for the boundary at  $x = 0$ , and

$$0 = [A(k) \cos(kL) + B(k) \sin(kL)] (m_L\ddot{\tau}(t; k) + \kappa_L\tau(t; k) + \delta m_L\dot{\tau}(t; k)) + [-A(k) \sin(kL) + B(k) \cos(kL)] kF_T\tau(t; k) \quad (5.16)$$

---

<sup>3</sup>There might be separable solutions to eq. (3.4) that do not satisfy the boundary conditions eqs. (5.7) and (5.8) individually but whose superposition does. Only looking for separable solutions that themselves satisfy the boundary conditions is a choice in the applied solution strategy.

for the boundary at  $x = L$ , after taking all terms to one side. This gives us two equations for  $A(k)$  and  $B(k)$  which we can simplify using eq. (5.9):

$$k \frac{F_T}{m_0} \frac{B(k)}{A(k)} - \frac{\kappa_0}{m_0} = \frac{\ddot{\tau}(t, k) + \delta \dot{\tau}(t, k)}{\tau(t, k)} = -k^2 c^2 \quad (5.17)$$

$$\frac{\left[ k \frac{F_T}{m_L} \cos(kL) + \omega_{bL}^2 \sin(kL) \right] \frac{A(k)}{B(k)} + \left[ \omega_{bL}^2 \cos(kL) - k \frac{F_T}{m_L} \sin(kL) \right]}{\cos(kL) + \frac{A(k)}{B(k)} \sin(kL)} = \frac{\ddot{\tau}(t, k) + \delta \dot{\tau}(t, k)}{\tau(t, k)} = -k^2 c^2 \quad (5.18)$$

This is where the choice to take  $\delta$  the same in eq. (5.3) as in eq. (3.4) comes in handy: because of this choice the time dependency in eqs. (5.17) and (5.18) can be eliminated using eq. (5.9). We can solve eq. (5.17) for  $\frac{B(k)}{A(k)}$  and absorb some constants in  $A(k)$  to obtain

$$\phi(x, k) = A(k) \sin(kx - \alpha(k)), \quad (5.19)$$

where

$$\alpha(k) = \arctan \left( -\frac{k F_T}{m_0 [\omega_{b0}^2 - k^2 c^2]} \right). \quad (5.20)$$

We can also combine eqs. (5.17) and (5.18) to eliminate  $\frac{B(k)}{A(k)}$ , which leaves us with an equation for the values of  $k$  for which the separable solutions  $\phi(x; k)\tau(t; k)$  indeed satisfy the boundary conditions eqs. (5.7) and (5.8):

$$k F_T [m_0 (k^2 c^2 - \omega_{b0}^2) + m_L (k^2 c^2 - \omega_{bL}^2)] \cos(kL) \quad (5.21a)$$

$$+ [k^2 F_T^2 - m_0 m_L (k^2 c^2 - \omega_{b0}^2) (k^2 c^2 - \omega_{bL}^2)] \sin(kL) = 0. \quad (5.21b)$$

This equation has only countably infinite solutions for  $k$ . Since  $k$  appears both inside and outside the sine and cosine functions, this equation is transcendental in such a way that a closed form solution is very hard if not impossible to find. Therefore, a numerical method could be implemented to approximate the roots of this equation.

Since eq. (5.21) only has countably infinite solutions, we can write our solution in terms of a sum of the found separable solutions:

$$u(x, t) = \sum_{n=1}^{\infty} \phi_n(x) [C_n \cos(\omega_n t) + D_n \sin(\omega_n t)] e^{-\frac{\delta}{2} t} \quad (5.22)$$

$$\phi_n(x) = \sin(k_n x - \alpha_n) \quad (5.23)$$

$$\alpha_n = \arctan \left( -\frac{k_n F_T}{m_0 [\omega_{b0}^2 - k_n^2 c^2]} \right) \quad (5.24)$$

$$\omega_n = 2\pi f_n = \sqrt{k_n^2 c^2 - \left(\frac{\delta}{2}\right)^2} \quad (5.25)$$

Here we absorbed  $A(k)$  in  $C(k)$  and  $D(k)$ . Note that eq. (5.21) having only countably infinite solutions also means that this model produces a discrete spectrum, just as in section 3.1.

The time dependent part can easily be shown to be the same as in the previous model using

$u_t(x, 0) \equiv 0$ :

$$\tau_n(t) = \sqrt{\frac{\delta^2}{4\omega_n^2} + 1} \cdot \sin(2\pi f_n t - \theta_n) e^{-\frac{\delta}{2}t} \quad (5.26)$$

$$2\pi f_n = \omega_n = \sqrt{k_n^2 c^2 - \left(\frac{\delta}{2}\right)^2} \quad (5.27)$$

$$\theta_n = \arctan\left(-\frac{2\omega_n}{\delta}\right), \quad (5.28)$$

so that leaves us with  $u(x, t) = \sum_{n=1}^{\infty} C_n \phi_n(x) \tau_n(t)$ .

### 5.1.3 A remark on the newly found basis

An unfortunate property of the  $\phi_n$  is that they are not orthogonal under the uniformly weighed integral inner product used in section 3.1. The equations 5.7 and 5.8 do not satisfy the requirements of a regular Sturm-Liouville problem mentioned in section 2.4 either, so we do not know of a way to find an inner product under which these eigenfunctions are orthogonal. An orthogonal basis can be constructed using the Gram-Schmidt procedure, see for instance Aliprantis et al. in chapter 6 of [12].

The inner product of the  $\phi_n$  with themselves are

$$\langle \phi_n, \phi_n \rangle = \frac{L}{2} - \frac{1}{4k_n} [\sin(2(k_n L - \alpha_n)) + \sin(2\alpha_n)], \quad (5.29)$$

and the inner product for two different eigenfunctions ( $n \neq m$ ) is

$$2 \langle \phi_n, \phi_m \rangle = \frac{\sin([k_n - k_m]L - (\alpha_n - \alpha_m)) + \sin(\alpha_n - \alpha_m)}{k_n - k_m} - \frac{\sin([k_n + k_m]L - (\alpha_n + \alpha_m)) + \sin(\alpha_n + \alpha_m)}{k_n + k_m}. \quad (5.30)$$

## 5.2 Influence on the spectrum

We are interested in the question whether the vibrating boundaries can account for shifts in the spectra of such a magnitude that it can cause beating with a frequency observed in the measurements. We therefore take a closer look at eq. (5.21) to see what we can say about the allowed values of  $k$  based on the parameters in this equation. To do that, we first make a series of substitutions in eq. (5.21):

- Rewrite  $kL = \pi\Lambda$ . Looking at eq. (5.23),  $\Lambda$  denotes the number of half homogeneous Dirichlet wavelengths (in space) present on the string for a certain mode.<sup>4</sup> The spatial homogeneous Dirichlet wavelength of the  $n$ -th mode is  $\frac{2L}{n}$ .
- Use  $m_s = \mu L = \frac{F_T L}{c^2}$  for the mass of the string between the bridge and the nut, using  $c^2 = \frac{F_T}{\mu}$  from section 3.1.
- Use  $c = 2L f_{\text{appr}}$  where  $f_{\text{appr}}$  is approximately  $f_1$ . This can be motivated with eq. (5.27), which shows that  $c \approx 2L f_1$  when  $\delta$  is small compared to  $f_1$ .

<sup>4</sup>Which makes  $\Lambda$  almost equivalent to  $n$  in the homogeneous Dirichlet case, but here  $\Lambda$  is not an integer.



- Rewrite  $\omega_{b0}$  and  $\omega_{bL}$  in terms of the above approximate frequency of the ground mode:

$$\omega_{b0} = 2\pi f_{\text{appr}} \omega_{r0}, \quad \omega_{bL} = 2\pi f_{\text{appr}} \omega_{rL}.$$

- Rewrite  $m_L$  in terms of  $m_0$ :  $m_L = m_0 m_{rL}$ . This means that  $m_{rL} = \frac{m_L}{m_0}$  is the ratio of the masses of the boundaries, which we assume to be of order 1.
- Rewrite  $m_s$  in terms of  $m_0$ :  $m_s = m_0 m_{rs}$ .

This results in the following equation:

$$-\frac{4\pi m_{rs} \Lambda [(1 + m_{rL})\Lambda^2 - (\omega_{r0}^2 + m_{rL}\omega_{rL}^2)]}{4\Lambda^2 m_{rs}^2 - \pi^2 m_{rL}(\Lambda^2 - \omega_{r0}^2)(\Lambda^2 - \omega_{rL}^2)} = \tan(\Lambda\pi). \quad (5.31)$$

Now we make an estimation of  $m_{rs}$ . We can calculate the mass of the string between the bridge and the nut by modelling it as a steel cylinder using the equation  $m_s = \frac{1}{4}\rho\pi d^2 L$ , where  $\rho$  is the density of steel and  $r$  the radius of the string. The string diameters and masses are shown in table 5.1, using  $\rho = 7.9 \text{ g/cm}^3$ . Since the mass of the guitar is in the order of a few kilograms,

Table 5.1: String diameters and masses between bridge and nut.

string name	$d$ (mm)	$m_s$ (g)
high E	0.20	0.16
B	0.25	0.25
G	0.41	0.67

we conclude that  $m_{rs}$  is in the order of  $10^{-4}$ .

Since we are interested explaining the beating of the largest amplitude change in the measurements, we look at those values of  $\Lambda$  that correspond to the modes with the highest amplitudes, which are in general the modes with the lowest frequencies. We therefore take  $\Lambda$  of order 1. We do not know much about the magnitude of  $\omega_{r0}$  and  $\omega_{rL}$ , but we assume them to be much larger than 1. This means that the left hand side of eq. (5.31) has the same order of magnitude as  $m_{rs}$ , which we found to be  $10^{-4}$ . With this order of magnitude we can use a linear approximation of the tangent function at the points  $n\pi$  to conclude that  $kL = \Lambda\pi = n\pi + \mathcal{O}(10^{-4})$ . Since  $k^2 c^2 \gg (\frac{\dot{\phi}}{2})^2$  the right hand side of eq. (5.23) is by very good approximation linear in  $k$ . From this we conclude that the influence of the co-vibrating boundaries on the frequencies of the modes is of the order 0.1% or smaller, which is too small to explain the approximate 1% shift in frequency which explains the beating on the frequency scale observed in the measurements.

The asymptotes of the left hand side shown in fig. 5.2 correspond to the eigenfrequencies of the string boundaries. This hints at a broader more complicated influence on the string motion: resonance with modes of the guitar body. The guitar body itself has a set of modes of its own, with a corresponding spectrum. An investigation of this effect falls beyond the scope of this text. It is however known that this effect is significant, since guitar builders carefully select the wood for the guitar body for its effect on the guitar sound.

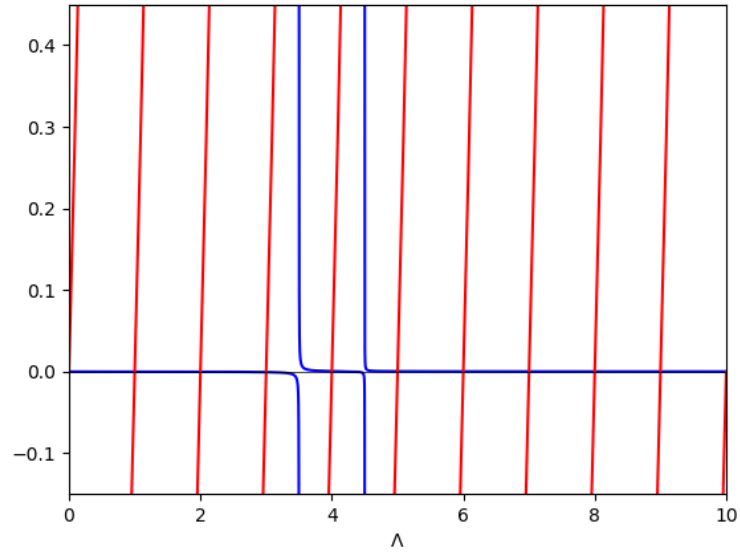


Figure 5.2: Plot of the left hand side (blue) and the right hand side (red) of eq. (5.31) as a function of  $\Lambda$ . The used parameter values are:  $m_{rs} = 10^{-4}$ ,  $m_{rL} = 0.2$ ,  $\omega_{r0} = 4.5$ ,  $\omega_{rL} = 3.5$ . Since  $m_{rs}$  is so small, the left hand side of eq. (5.31) will be very close to zero apart from a very small neighborhood around the singularities. Therefore the solutions to eq. (5.31) are very close to  $n\pi$  and thus the  $k_n$  very close to  $\frac{n\pi}{L}$ .



## Chapter 6

# Rotation of the plane of string vibration

In section 5.6 of [2] it is mentioned by Fletcher et al. that non-linear effects in the string cause exchange of energy between the parallel and perpendicular modes. According to them this exchange in energy happens in such a way that each point on the string moves in a plane that is itself rotating around the equilibrium position of the string with a frequency of around 1 Hz (called the angular precession velocity by Fletcher et al.). In this chapter we do a brief investigation of this effect, by assuming that the solution  $u$  from the previous model (that of chapter 3) describes the radial direction of the string, where the plane of oscillation is assumed to rotate with constant speed around the axis along the equilibrium position of the string. This is a simplification with respect to Fletcher et al., since they mention that the rotation speed of this plane is dependent on the mode.

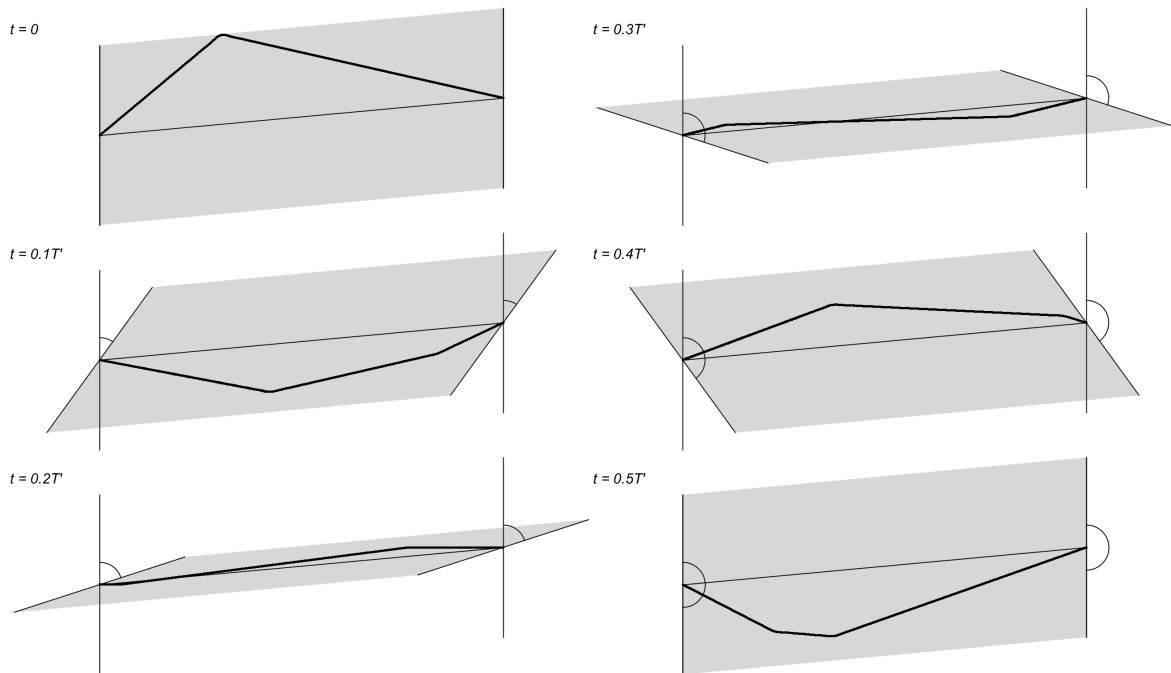


Figure 6.1: Rotation of the plane of oscillation. The gray area shows the orientation of the plane, and the circle arcs on either side denote the angle this plane has rotated over time. The oscillation plane here rotates with a period of  $T' = \frac{2\pi}{\Omega} = 0.2\text{ s}$ , where  $\Omega$  is the angular velocity of the rotating plane. The string moves according to the model with homogeneous Dirichlet boundary conditions with  $\delta = 4\text{ s}^{-1}$  and  $f_1 = 329.63\text{ Hz}$ , the ground frequency of the high E string.

## 6.1 Derivation of the new signal model

We now describe the motion of the string by:

$$\mathbf{u}(x, t) = u(x, t)\hat{\mathbf{r}}(t), \quad (6.1)$$

where  $\hat{\mathbf{r}}$  is a unit vector that rotates with an angular velocity  $\Omega$  in the 2D plane:

$$\hat{\mathbf{r}}(t) = (\cos(\Omega t), \sin(\Omega t)). \quad (6.2)$$

Hence  $\mathbf{u} = (u^\parallel, u^\perp)$  is now a function to  $\mathbb{R}^2$ :

$$\mathbf{u} : [0, L] \times [0, \infty) \rightarrow \mathbb{R}^2. \quad (6.3)$$

We construct a new model of the output signal of the string:

$$S(t) := S_1^\parallel u_t^\parallel(x_{\text{pu}}, t) + \left[ S_1^\perp + S_2^\perp u^\perp(x_{\text{pu}}, t) \right] u_t^\perp(x_{\text{pu}}, t). \quad (6.4)$$

Here the first term is the contribution of the motion of the string parallel to the fret board, analogous to the previous model of the pickup signal. The second term is the contribution of the motion of the string orthogonal to the fret board, where a linear dependence on the displacement of the string is included. Since we expect the signal to be weaker if the string is further away from the pickup, we take  $S_2^\perp < 0$ .

Substituting the series solution of  $u$  gives in eq. (6.4):

$$S(t) = S_1^\parallel [\cos(\Omega t)u_t(x_{\text{pu}}, t) - \Omega \sin(\Omega t)u(x_{\text{pu}}, t)] \quad (6.5a)$$

$$+ \left[ S_1^\perp + S_2^\perp \sin(\Omega t)u(x_{\text{pu}}, t) \right] [\sin(\Omega t)u_t(x_{\text{pu}}, t) + \Omega \cos(\Omega t)u(x_{\text{pu}}, t)] \quad (6.5b)$$

$$= e^{-\frac{\delta}{2}t} \left[ \sum_{n=1}^{\infty} A_{n1} \cos([\omega_n - \Omega]t - \Theta_{n1}) \quad (6.5c)$$

$$- \sum_{n=1}^{\infty} A_{n2} \cos([\omega_n + \Omega]t - \Theta_{n2}) \right] \quad (6.5d)$$

$$+ e^{-\delta t} \left[ \sum_{n=1}^{\infty} \sum_{m=1}^{\infty} B_{nm3} \sin((\omega_n - \omega_m - \Omega)t - \Theta_{nm3}) \quad (6.5e)$$

$$- \sum_{n=1}^{\infty} \sum_{m=1}^{\infty} B_{nm4} \sin([\omega_n - \omega_m + \Omega]t - \Theta_{nm4}) \quad (6.5f)$$

$$+ \sum_{n=1}^{\infty} \sum_{m=1}^{\infty} B_{nm5} \sin([\omega_n + \omega_m - \Omega]t - \Theta_{nm5}) \quad (6.5g)$$

$$- \sum_{n=1}^{\infty} \sum_{m=1}^{\infty} B_{nm6} \sin([\omega_n + \omega_m + \Omega]t - \Theta_{nm6}) \right], \quad (6.5h)$$

for certain constants

$$A_{n1}, A_{n2} \propto C_n \phi_n(x_{\text{pu}}) \sqrt{(S_1^\parallel)^2 + (S_1^\perp)^2} \quad (6.6)$$

$$B_{nm3}, B_{nm4}, B_{nm5}, B_{nm6} \propto S_2^\perp C_n C_m \phi_n(x_{\text{pu}}) \phi_m(x_{\text{pu}}) \quad (6.7)$$

and phase shifts  $\Theta_{n1}, \dots, \Theta_{n6}$ . We are not interested in the exact values of the phase shifts (because as we discussed in section 2.1, the phase shift is of relatively little importance to the sound of the guitar). We also do not go into the details of calculating the coefficients  $A_{n1}$ ,  $A_{n2}$  and  $B_{nm3}, \dots, B_{nm6}$  since these calculations get quite long and messy and we are for now merely interested in the qualitative properties of the wave form produced by this model.

## 6.2 Properties of the new signal model

For simplicity, we look at the properties of this solution in the case that there is only a single mode excited on the string:

$$S(t) = e^{-\frac{\delta}{2}t} \left[ A_{n1} \cos([\omega_n - \Omega]t - \Theta_{n1}) - A_{n2} \cos([\omega_n + \Omega]t - \Theta_{n2}) \right] \quad (6.8a)$$

$$+ e^{-\delta t} \left[ B_{nn3} \sin(-\Omega t - \Theta_{nn3}) - B_{nn4} \sin(\Omega t - \Theta_{nn4}) \right] \quad (6.8b)$$

$$+ B_{nn5} \sin([2\omega_n - \Omega]t - \Theta_{nn5}) - B_{nn6} \sin([2\omega_n + \Omega]t - \Theta_{nn6}) \Big]. \quad (6.8c)$$

We see that the rotation velocity of the plane  $\Omega$  acts as the small difference in frequency between different modes that causes beating in the way we described in section 3.4. The coefficients  $S_1^{\parallel}$ ,  $S_1^{\perp}$  and  $S_2^{\perp}$  can be tuned to reflect the effect that perpendicular modes get detected far weaker than parallel modes by the pickup, as mentioned by Horton et al. in [8].

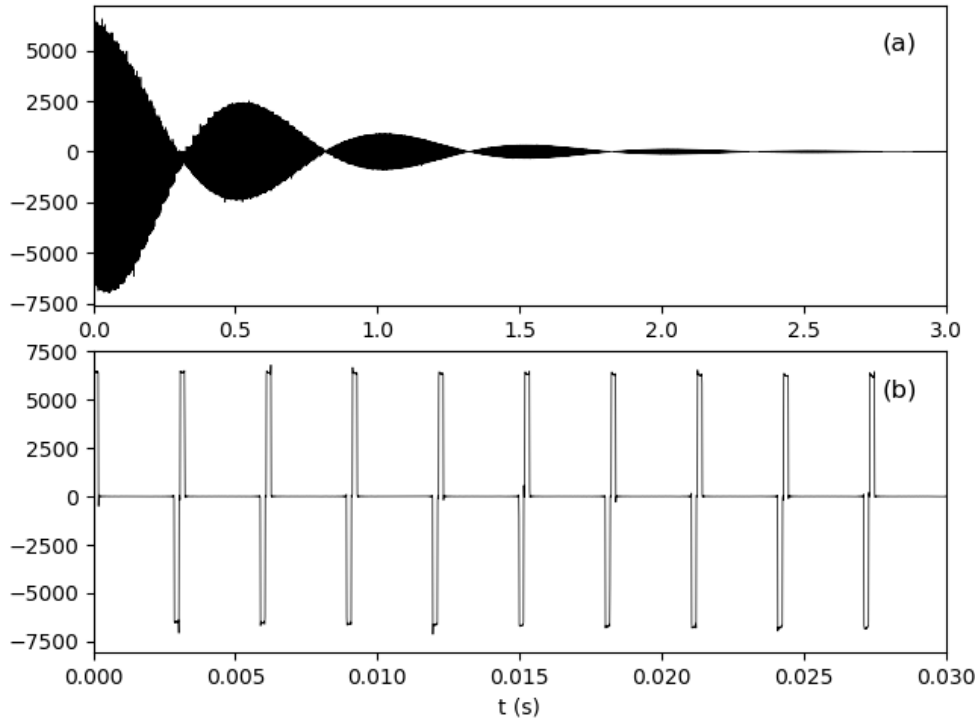


Figure 6.2: Plot of the model of the output signal from an electric pickup sensing a string that vibrates in a slowly rotating plane. Parameter values:  $\delta = 4$ ,  $\Omega = 2\pi$ ,  $f_1$  for the high E string,  $S_1^{\parallel} = 1$ ,  $S_1^{\perp} = \frac{1}{2}$ ,  $S_2^{\perp} = -\frac{1}{2}$ , 1000 modes.

## 6.3 Predicted signal

In figs. 6.2 and 6.3 we see the result of this new model for the pickup signal for respectively  $\Omega = 2\pi$  and  $\Omega = 20\pi$ . The other parameters used here are  $\delta = 4$ ,  $f_1$  for the high E string (see table 2.1),  $S_1^{\parallel} = 1$ ,  $S_1^{\perp} = \frac{1}{2}$ ,  $S_2^{\perp} = -\frac{1}{2}$ , using 1000 modes.

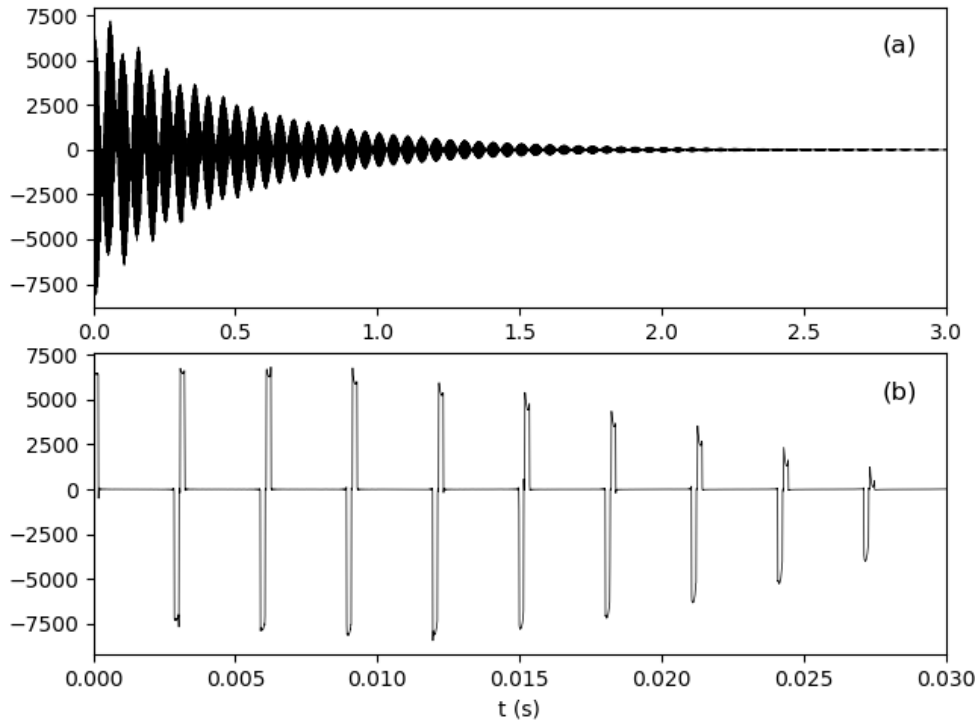


Figure 6.3: Plot of the model of the signal that includes rotation of the plane of oscillation. Parameter values:  $\delta = 4$ ,  $\Omega = 20\pi$ ,  $f_1$  for the high E string,  $S_1^{\parallel} = 1$ ,  $S_1^{\perp} = \frac{1}{2}$ ,  $S_2^{\perp} = -\frac{1}{2}$ , 1000 modes.

We now clearly see that the predicted signal contains beating and is asymmetric around its equilibrium position, at least for the chosen values of  $S_1^{\parallel}$ ,  $S_1^{\perp}$  and  $S_2^{\perp}$ . These parameter values were chosen by trial and error to show that this model can reproduce some of the effects observed in the measurements.

Looking at these plots, it becomes more likely that introducing beating in this way can reproduce some of the complexity seen in the measurements. A suitable next step would probably be to make the angular precession velocity mode dependent, so that beating will occur on various time scales.

# Chapter 7

## Conclusion and discussion

### 7.1 Findings

#### 7.1.1 Background

The study presented in this text was motivated by the suggestion of Erich Andreas in his YouTube video *Gibson Les Paul Vs Fender Stratocaster - Which One Is Better?* that the timbre of an electric guitar mainly depends on its scale length. There is a large amount of literature on the working of stringed instruments like *The physics of musical instruments* by Fletcher et. al [2] and more specifically on electric guitars [7, 8].

#### 7.1.2 Basic model of the guitar, capturing the most essential ingredients

Inspired by the main features of measured waveforms (with a Fender Lead III built in 1982), during the research as described in this report we focused on two aspects of this waveform: damping and beating (a low frequency amplitude modulation), based on predictions made by Fletcher et al. in section 5.6 of [2].

After a literature survey, we opened our own investigation in chapter 3 by exploration of probably the simplest possible model of an electric guitar that still captures some of the most essential ingredients of this instrument, namely:

- a) It consists of a vibrating string with essentially fixed ends; we allow only transverse vibrations, in only one dimension.
- b) The string is released from an initially approximately triangular shape; the position of the top of this triangle can be specified.
- c) The vibration of the string is weakly damped, so that a produced tone will be audible for only a limited period of time.
- d) The actual signal produced comes from an electromagnetic pick-up, which measures the motion of only a very limited and well defined portion of the vibrating string; the position of the pick-up turned out to be an important parameter.
- e) the signal produced is proportional to the velocity of the observed portion of the string.

This model makes two general predictions about the timbre of the electric guitar:

- The closer the used pickup of the e-guitar is to the bridge, the fuller the spectrum is and the stronger the overtones at the high end of the auditory range (up to around 20 kHz) are present. This corresponds to the experience of guitarists that the closer the used pickup is to the bridge, the sharper the sound produced by this pickup is.
- The waveform and its corresponding spectrum only depend on the relative position of the pickup and pluck position on the string. This means that the model predicts that if we were to scale the string length, the distance from the bridge to the pickup and the distance from the bridge to the plucking position all with the same factor, the waveform



and its corresponding spectrum would not change. This prediction was not tested against measured data.

### 7.1.3 The damping parameter: explanation of the loss of amplitude over time, refutation of the hypothesis that it can explain the envelope modulation

In chapter 4 we compared the model from chapter 3 with measurements of the signal of an electric guitar. We did this by making fits to the envelopes of these measured signals and looking at their spectra. From this we learned:

- The measurements with a pickup closer to the bridge show beating with a higher frequency than those with a pickup further away from the bridge. A possible explanation for this is that the pickup position influences the strength with which modes get detected. This means that the mode number whose difference between the parallel and perpendicular modes dominates the beating in the wave form depends on the pickup location.
- The damping parameter  $\delta$  can roughly explain the shape of the envelope of the measured signals. The signals show that a damping term in the wave equation for the string is certainly needed.
- The order of magnitude of the parameter  $\delta$  that best fits the envelope of the measured signals does not have a big enough effect on the spectrum to obtain the anharmonicity of the spectra of the measurements. The measured deviation from an harmonic spectrum is also more complex than the model can predict. These measured deviations for instance are sometimes negative, which the model cannot account for.
- Based on the previous point, we conclude that, as far as the electric guitar is concerned, the observed beating cannot be explained by damping through a possible mechanism as suggested by Gough and as paraphrased by Fletcher and Rossing [2, Sec 5.6]. According to this explanation, beating would be the result of perpendicular and parallel modes on the string having slightly different effective values of  $\delta$  resulting in them having slightly different frequencies. To explain beating we need an effect that can produce a shift of the frequencies in the spectrum in the order of 1% in the lower end of the spectrum, because only the presence of those modes is strong enough to account for the observed beating. The values of  $\delta$  obtained in the fits can only account for shifts of order  $10^{-4}\%$ ,  $10^{-4}\%$  and  $10^{-5}\%$  for the high E, B and G strings respectively.

### 7.1.4 Refutation of co-vibrating boundaries hypothesis as explanation of the envelope modulation

Since we concluded that the parameter  $\delta$  can not explain the deviation from harmonic spectra and beating, in chapter 5 we included co-vibrating string boundaries into the model, after a suggestion of Fletcher et al. in section 5.6 of [2] that this could explain beating. An interesting theoretical result of these calculations is that this relaxation of the Dirichlet boundary conditions resulted in a basis that is no longer orthogonal under the standard inner product used for the standard Fourier series given by  $\langle f, g \rangle = \int_0^L f(x)g(x)dx$ . We derived an equation for the eigenvalues dependent on the masses and angular frequencies of the boundaries, and also the masses of the string and the guitar itself. From this equation we concluded that the frequencies of the modes on the string are also not shifted enough by the influence of the oscillating boundaries to explain the measured deviation from an harmonic spectrum or the observed beating. The

inclusion of the co-vibrating boundaries can namely only account for shifts in the spectrum in the order of 0.1%. This research however did hint on the influence on the guitar sound of the spectrum of the guitar body itself.

### 7.1.5 Explanation of the envelope modulation by interaction of 3D motion and pickup characteristics

From our results of chapter 4 and chapter 5, in which we have shown that the beating observed in the electric guitar signal cannot be explained by the effect of damping on the eigenfrequencies, nor by the impact of co-vibrating boundaries on these, we conclude that the explanation of this effect must be more advanced. Fletcher et al. describe an alternative effect in section 5.6 of [2] that could explain beating. They propose that non-linear effects in the string cause exchange of energy between the parallel and perpendicular modes. This exchange in energy is in such a way that each point on the string moves along an ellipse that is itself rotating around the equilibrium position of the string with a frequency of around 1 Hz. In chapter 6 we did a brief investigation of this effect, by assuming that the solutions  $u$  from the previous models describe the radial direction of the string, where the plane of oscillation is assumed to rotate with constant speed around the axis along the equilibrium position of the string. Combined with a simple model for the interaction of the string with the pickup element of the guitar, this produced signals with beating that show qualitative resemblance to the measurements. In the model, the angular velocity of the aforementioned plane acts as the shifts in the spectrum we expect to see to explain beating.

## 7.2 Emerged questions

During the research for this text, the following questions and recommendations for further research into the topic emerged.

- Concerning experimental data: To better isolate the influence of certain parameters of the process from guitar pluck to output signal (specifically how the damping and beating present themselves in the waveform), the plucking of the strings should be more controlled, mainly the force with which the string gets plucked. This is needed because as suggested Fletcher et al. in [2, Sec 5.6] and briefly investigated in chapter 5, the cause of the beating might lie in non-linear effects on the string, which generally depend on the exact amplitude of the string.
- An investigation could be done into which shapes and patterns in the spectrum result in beating in the waveform of the output signal. Then the shapes and patterns in the spectrum that do indeed cause beating could be linked to properties of the electric guitar.
- The investigation into the rotation of the plane of vibration could be extended in the way it was originally suggested by Fletcher et al. in section 5.6 of [2], by making the angular velocity of the plane of vibration mode dependent. This could possibly give an insight in some of the more complex non-periodic beating patterns in the measurements.
- In [8], Horton et al. mention that the signal produced by modes parallel to the fret board have (approximately) twice the frequency of the signal produced by the corresponding perpendicular mode. This is because the detection of the pickup of the motion of the string is symmetric around the equilibrium position of the string for parallel modes, but not for perpendicular modes. This has potentially profound implications for the results presented in this text, because this process might suggest that the string only needs half

the vibration frequency to produce a certain note as compared to the vibration frequency predicted by the models in this text (although the model in section 3.1 shows that the motion of the string is not exactly symmetric around the equilibrium position of the string).

- It was shown that the signal produced by an electrical guitar is dependent on the plane in which the string vibrates (or a more complicated extension of this concept, see chapter 6). It could therefore be insightful to compare measurements of the signal of an electric guitar to measurements of the sound of an acoustic guitar. This is because for acoustic guitars this influence of the direction of the vibration of the strings on the sound the guitar produces is not present, or at least not in the same way.

# Appendix A

## Measurements

See the following pages for the wave forms and the spectra of the measurements.

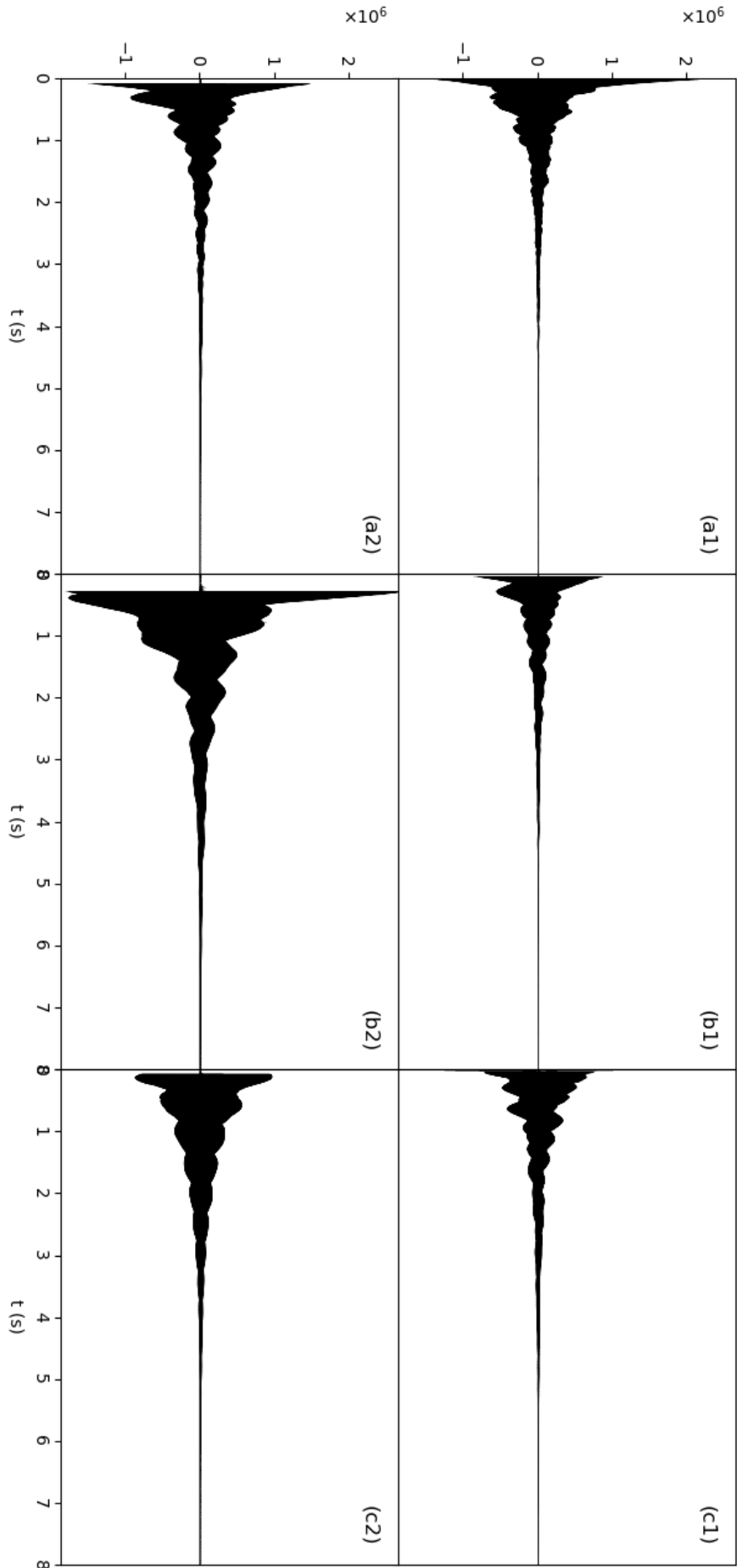


Figure A.1: Signals produced by plucking the high E string. Plucked at  $x_{pu1}$  (a),  $x_{pu2}$  (b) and  $L/2$  (c), using pickup 1 (1) and pickup 2 (2).

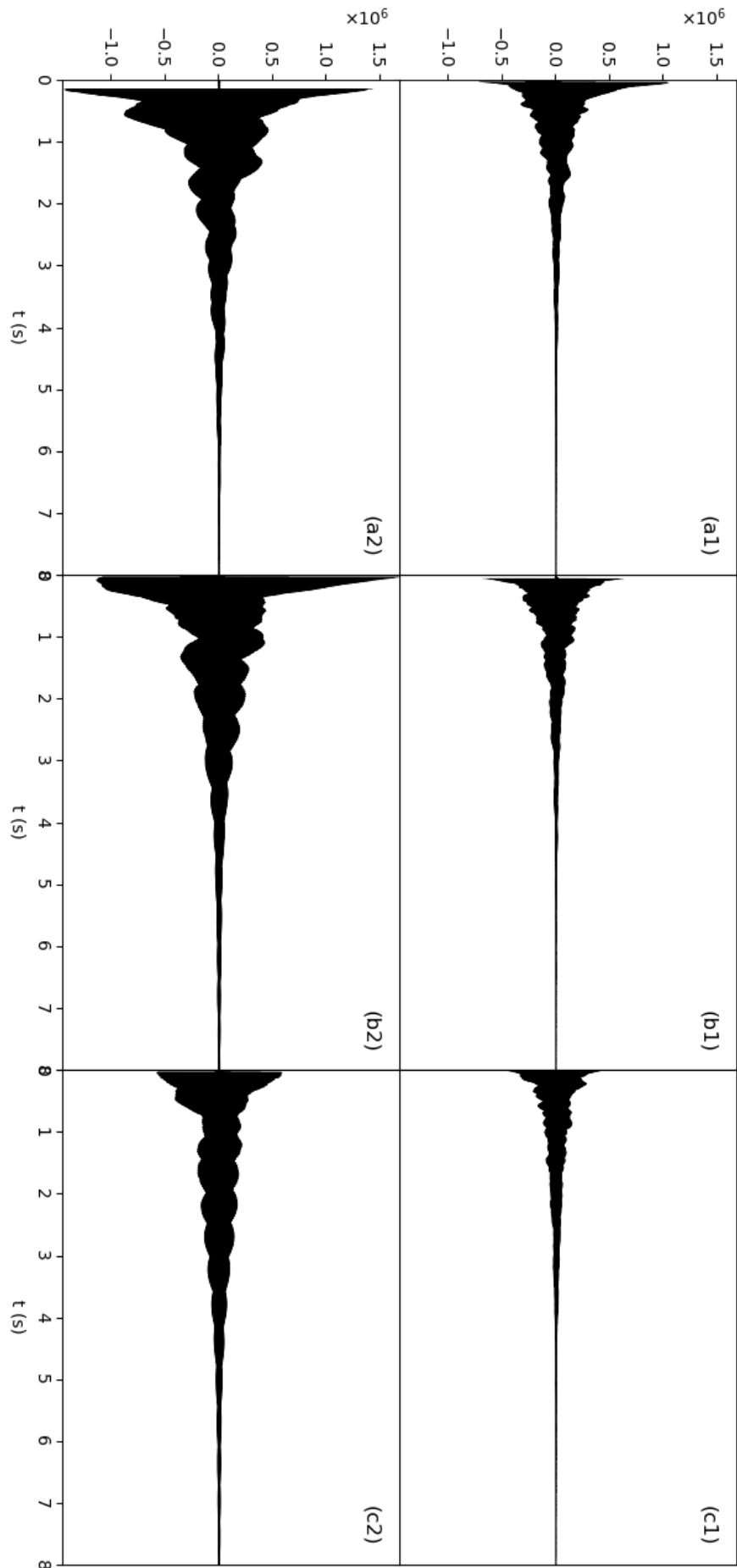


Figure A.2: Signals produced by plucking the B string. Plucked at  $x_{pu1}$  (a),  $x_{pu2}$  (b) and  $L/2$  (c), using pickup 1 (1) and pickup 2 (2).

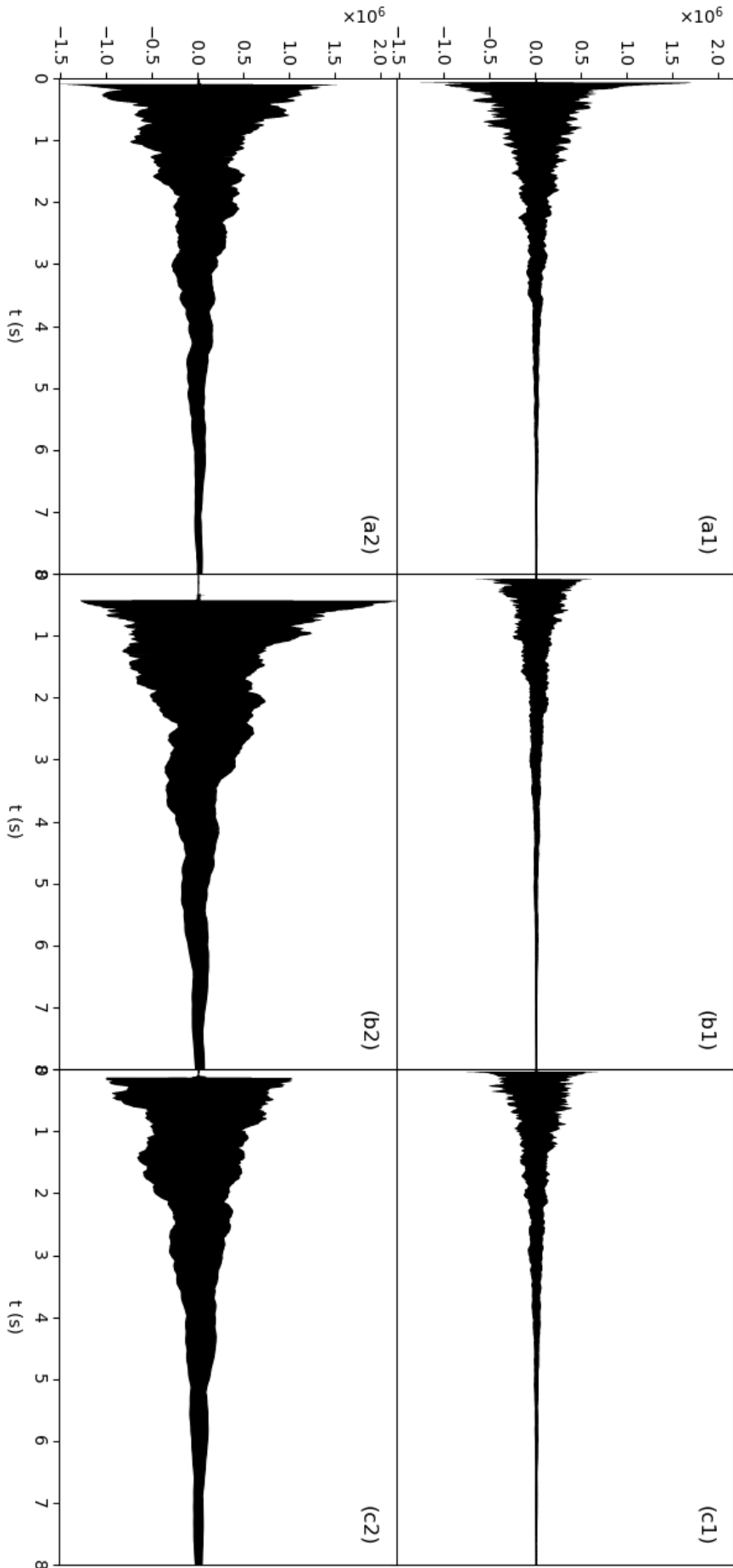


Figure A.3: Signals produced by plucking the G string. Plucked at  $x_{pu1}$  (a),  $x_{pu2}$  (b) and  $L/2$  (c), using pickup 1 (1) and pickup 2 (2).

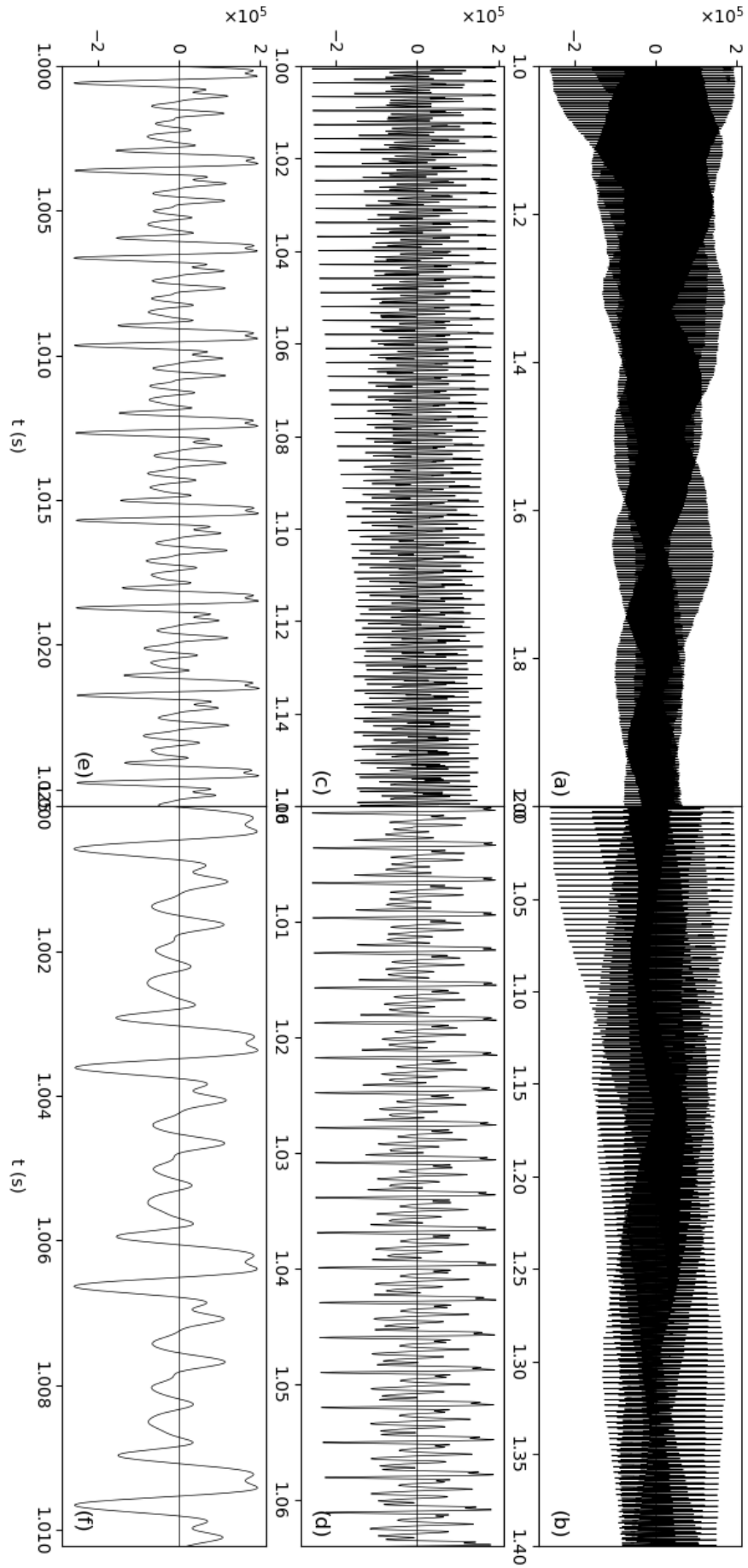


Figure A.4: Signal produced by plucking the high E string plucked at  $x_{pu1}$  using pickup 1, shown at various time scales.



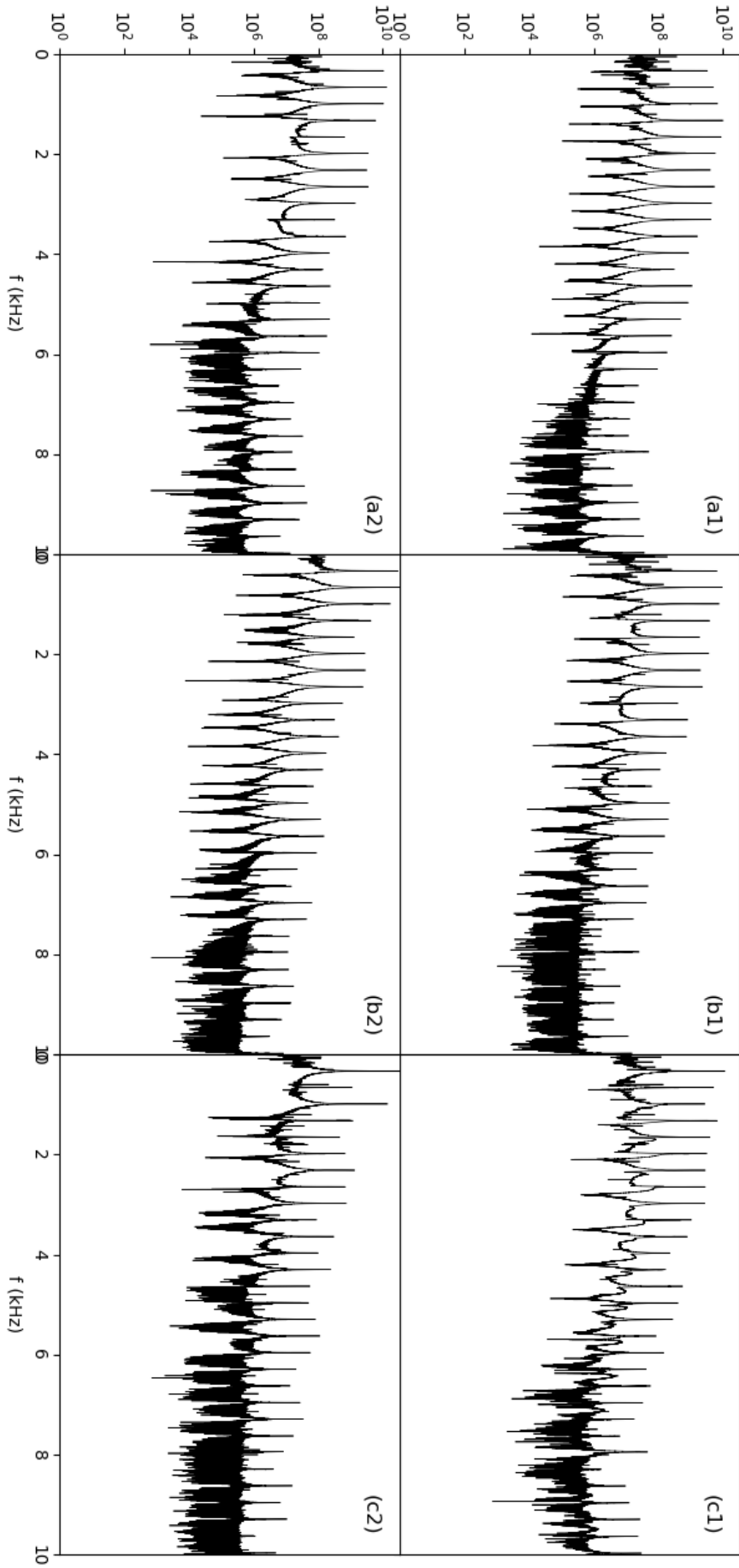


Figure A.5: Spectra of the signals produced by plucking the E string. Plucked at  $x_{pu1}$  (a),  $x_{pu2}$  (b) and  $L/2$  (c), using pickup 1 (1) and pickup 2 (2).

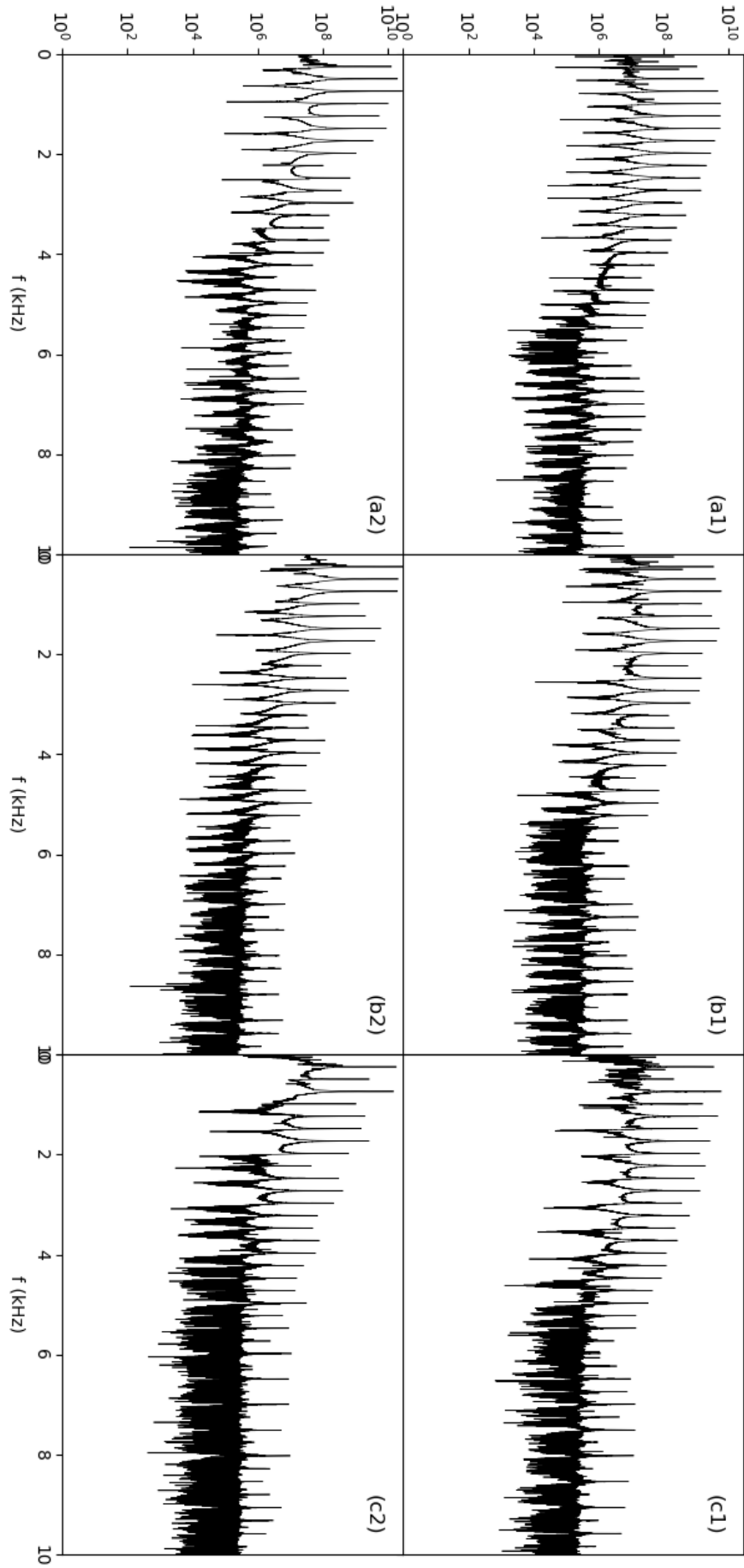


Figure A.6: Spectra of the signals produced by plucking the B string. Plucked at  $x_{pu1}$  (a),  $x_{pu2}$  (b) and  $L/2$  (c), using pickup 1 (1) and pickup 2 (2).

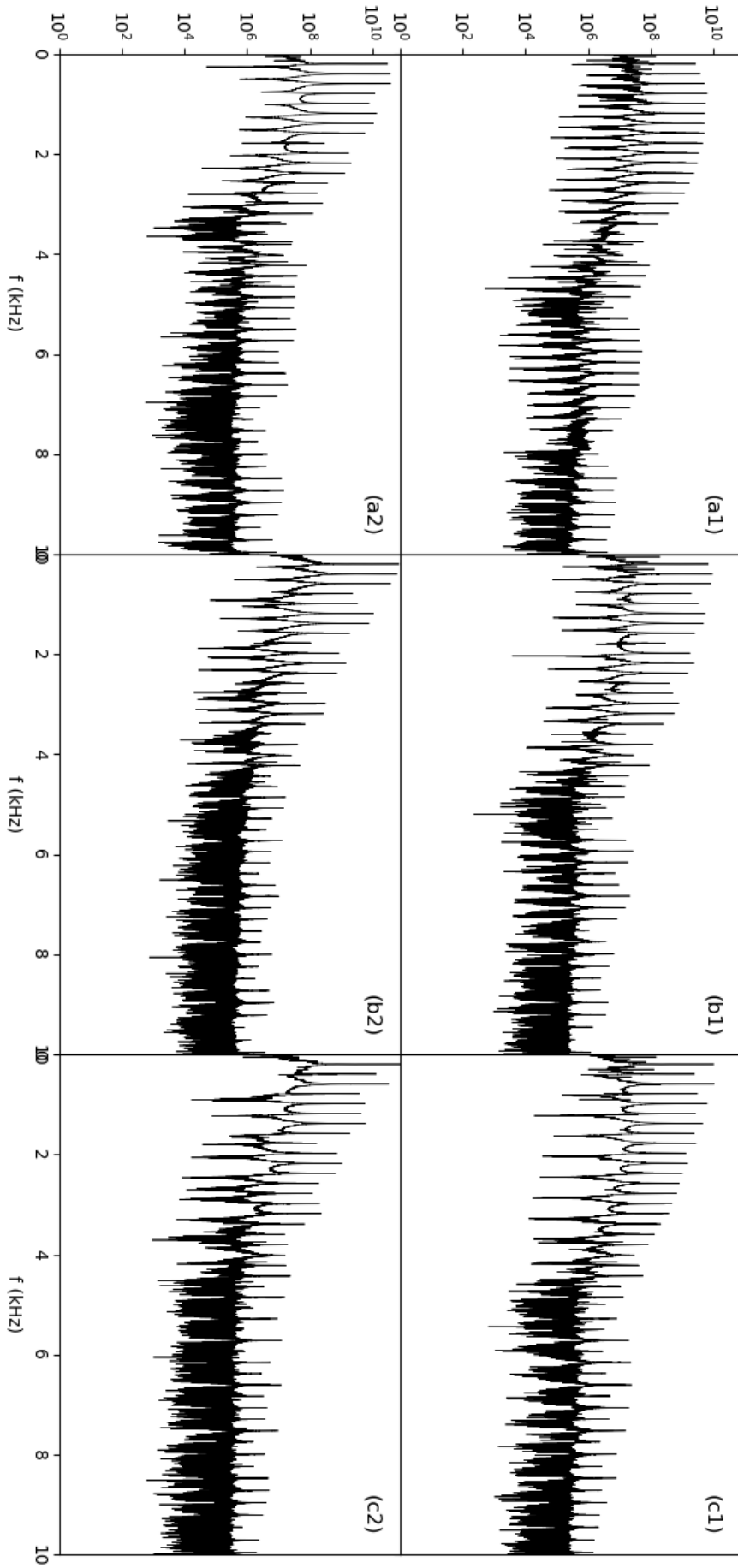


Figure A.7: Spectra of the signals produced by plucking the G string. Plucked at  $x_{pu1}$  (a),  $x_{pu2}$  (b) and  $L/2$  (c), using pickup 1 (1) and pickup 2 (2).

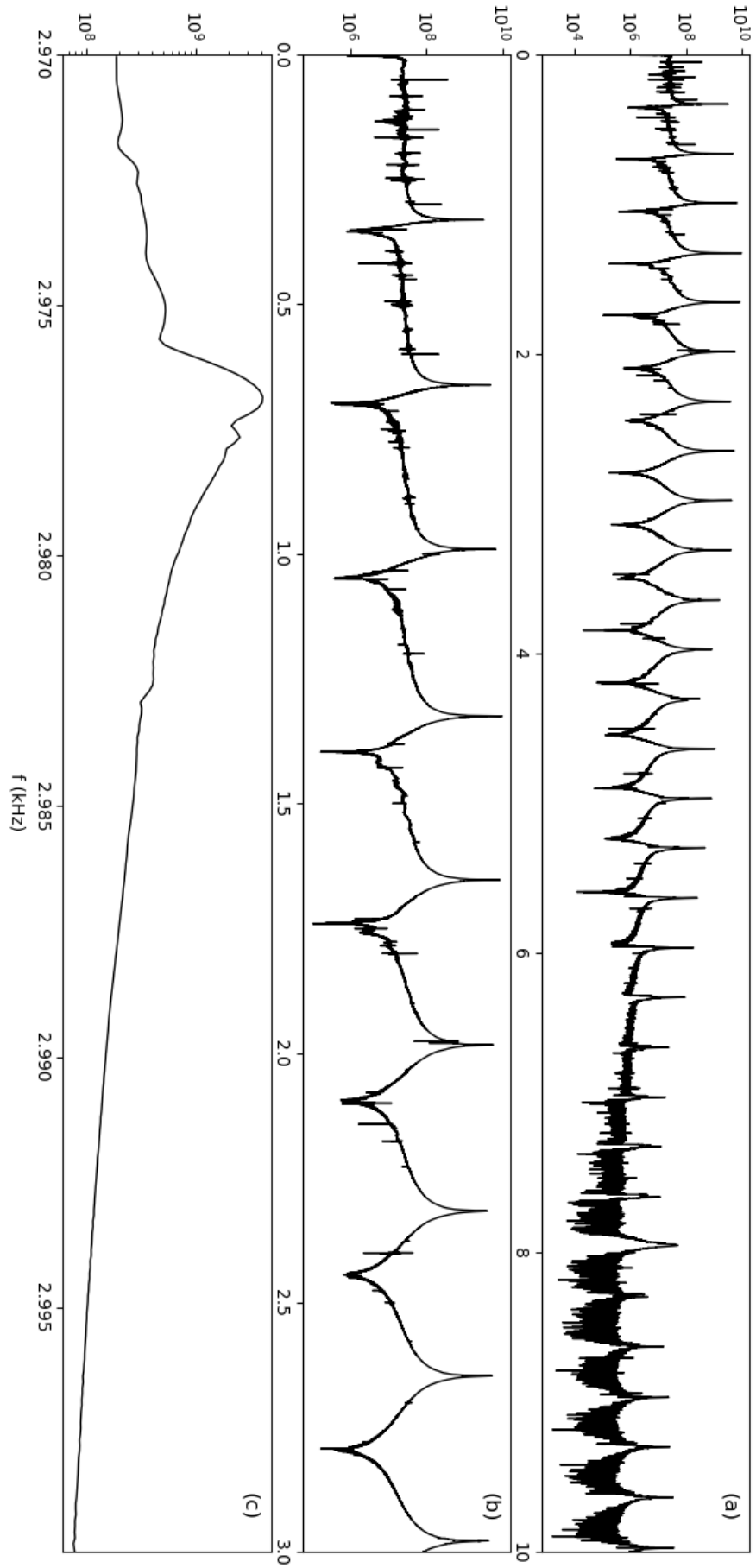


Figure A.8: Spectrum of the signal produced by plucking the high E string plucked at  $x_{pu1}$  using pickup 1, shown at various time scales.



# Appendix B

## Information content: WAV files

The WAV file (denoted by the file extension .wav) is a standard for digitally storing sound. A WAV file is essentially an array of numbers called samples, each of which tells the cone of a speaker in which position it should be at a certain point in time. The WAV file is characterised by the following parameters:

- The number of audio channels: 1 channel is called mono, 2 channels is called stereo. The array of the WAV file consists of first a concatenation of the samples of all the channels at the first point in time, then this concatenation of the samples of all the channels at the second point in time, and so on (so multiple channels are not stored each in a separate array).
- The sample width in bytes: This specifies how much memory is used to specify each sample. A sample width of  $n$  says that the sample is specified by  $8n$  bits which combined have  $(2^8)^n$  different possible states. Since the stored value is signed (i.e. can be both positive and negative), the amplitude is specified with an accuracy of  $(2^8)^{n-1} - 1$  possible values.
- The frame rate or sample rate: This specifies how many samples there are in a second. Popular industry standards are 44.1 kHz and 96 kHz.
- The total number of frames in the array.
- The compression type: in this research no compression was used [13].

Note that the sample rate limits the range of frequencies your audio file can contain. To create the simplest waveform of frequency  $f$ , a block wave, you need a sample frequency of at least  $2f$  to make a distinction between the maximum and minimum displacement. Therefore the highest frequency oscillation the WAV file can contain is limited by half the sample rate. This also explains the industry standard of 44.1 kHz, since the highest frequency sound people can perceive is around 20 kHz.



# Bibliography

- [1] Andreas, E. [YourGuitarSage]. (2017, February 17). *Gibson Les Paul Vs Fender Stratocaster - Which One Is Better?* [Video file]. Retrieved from <https://www.youtube.com/watch?v=nSMfMqfJ13o>
- [2] Fletcher, N. H., Rossing, T. D. (2012). *The physics of musical instruments*. Springer Science & Business Media.
- [3] OpenStax. Section 17.6: Hearing. In *Introduction to Science and the Realm of Physics, Physical Quantities, and Units*. Retrieved from <https://courses.lumenlearning.com/physics/chapter/17-6-hearing/>
- [4] Starlin, M. (Retrieved 2019). Electric guitar parts. Retrieved from: <http://www.markstarlin.com/guitar/2014/8/28/guitar-parts>
- [5] Štěpánková, I. (2017). *The Effect of Phase Spectrum on Auditory Perception*. Retrieved from [http://poseidon2.feld.cvut.cz/conf/poster/proceedings/Poster\\_2017/Section\\_NS/NS\\_011\\_Stepankova.pdf](http://poseidon2.feld.cvut.cz/conf/poster/proceedings/Poster_2017/Section_NS/NS_011_Stepankova.pdf)
- [6] The SciPy community (2019, Januari 31). *Discrete Fourier Transform (numpy.fft)*. Retrieved from: <https://docs.scipy.org/doc/numpy/reference/routines.fft.html>
- [7] Perov, P., Johnson, W., Perova-Mello, N. (2015). *The physics of guitar string vibrations*. American journal of physics, 84(1), 38-43.
- [8] Horton, N. G., & Moore, T. R. (2009). *Modeling the magnetic pickup of an electric guitar*. American journal of physics, 77(2), 144-150.
- [9] Fletcher, N. H. (1976). *Plucked strings - a review*. Catgut Acoust. Soc. Newsletter, 26, 13-17.
- [10] Haberman, R. (2012). *Applied partial differential equations with Fourier series and boundary value problems*. Essex, England: Pearson Higher Ed.
- [11] Vuik, C., Vermolen, F.J., van Gijzen, M.B., Vuik, M.J. (2016). *Numerical Methods for Ordinary Differential equations*. Delft: Delft Academic Press/VSSD.
- [12] Aliprantis, C.D, Burkinshaw, O. (1998). *Principles of Real Analysis*. London, England: Academic Press Limited.
- [13] Python Software Foundation (2019, July 18). *wave — Read and write WAV files*. Retrieved from: <https://docs.python.org/3/library/wave.html>